Inception and evolution of La Corona lava tube system (Lanzarote, Canary Islands, Spain)

I. Tomasi[1], M. Massironi[1], C.M. Meyzen[1], R. Pozzobon[1,2], F. Sauro[3], L. Penasa[1,2], T. Santagata[4], M. Tonello[1], G. D. Santana Gomez[5] and J. Martinez-Frìas[6]

[1]Department of Geosciences, University of Padua, Italy;

[2] INAF - Osservatorio Astronomico di Padova, Italy

[3]Department of BiGeA, University of Bologna, Italy;

[4]Virtual Geographic Agency (VIGEA), Reggio Emilia, Italy;

[5]Vulcan Vertical Espeleologiasy Barrancos;

[6]Instituto de Geosciences - IGEO (CSIC-UCM), Madrid, Spain

Corresponding author: Ilaria Tomasi (ilaria.tomasi.2@phd.unipd.it)

Key Points:

- The presence of a weak pyroclastic layer in pre-existing lava flows favours the enlargement of lava tubes on Earth.
- The excavation process of lava tubes is enhanced by the thermo-mechanical erosional action of molten lavas at bedrock knickpoints.
- The large lava tube at La Corona may provide analogues for extra-terrestrial lava tube structures.

Abstract

Growing interest in studying large terrestrial lava tubes is motivated in part by their analogy with their extra-terrestrial counterparts. However, on Earth, the formation of such structures is still poorly understood. Here, the lava tube system of La Corona (Lanzarote, Canary Islands, Spain) is studied to identify how pre-existing stratigraphy can govern a lava tube's evolution. Combining terrestrial laser scanner (TLS) technology with field observations and geochemical analyses of the pre-existing lava enabled us to reconstruct the three-dimensional geometry of the lava tube system, the paleo-surface trough which it developed, and the volcanic series into which it carved its path. We show that a pyroclastic layer played a key role in the development of the lava tube. The layer - derived from late Quaternary Strombolian activity - is traceable along almost the full length of the tube path and defines the paleo-topography. The excavation process mostly happens because of the mechanical strength of the substrate, that controls the widening of the growing lava tube. Other influential parameters controlling erosion include slope variations of the paleo-surface (i.e., knickpoints), and the lava physical properties. Since weak layers such as regolith are a common feature of extra-terrestrial lava flows, the processes seen at La Corona to the may be highly relevant to the development of planetary lava tube systems.

Plain Language Summary

Lava tubes are a promising subject for future planetary exploration. Within this framework, improved knowledge of how these lava caves form and evolve in the post-cooling phase is crucial. The best way to achieve such insights is to focus on their terrestrial analogues on volcanic islands (i.e., Canary Islands, Hawai'i, Iceland, etc.). Here we study the large lava tube complex of La Corona (Lanzarote, Canary Islands) to constrain the different stages of its development. Its genesis depended on the presence of a weak pyroclastic layer, favouring its initial emplacement. Its subsequent development depended largely on the duration of the thermal contact and the mechanical interaction between molten lavas and pre-existing lava flows, as well asthe paleo-topography emphasisedby the pyroclastic layer and also by the chemical and physical properties (e.g. solidity, state of weathering) of the pre-existing lava pile. The presence of a weak layer as observed at the La Corona tube system is of interest for understanding the processes by which extra-terrestrial lava tubes develop among lava sequences where weak layers such as ash layer, rubble and complex ancient surface are likely to be commonly found.

1 Introduction

During effusive volcanic eruptions lava tubes work as thermally efficient conduits, where the minimization of heat loss allows the transport of lava flows over long distances up to several tens of kilometres. Ultimately, the length of a lava tube will be controlled mainly by the duration of the eruption, effusion rates, and thermal efficiency and stability of the lava tube system (Hon et al., 1994; Peterson et al., 1994; Keszthelyi and Self, 1998; Pasquarè et al., 2008; Kempe et al., 2010).

Two main modes of development have been reported for these structures: 1) *crusting over* , when the roof is formed at the top of a lava channel by obstruction and/or levee accretion; and 2) *inflation*, when lava is injected below previously cooled lava sheets (Bravo, 1964; Greeley et al. 1971b; Greeley and Hyde, 1972; Francis, 1993; Hon et al., 1994; Kempe et al., 2010). At first inflation acts within thin sheets of lava, but then the pathway can evolce into elliptical lava tube systems as described by Cooper and Kauahikaua (1992) or as *deep inflation* by Sauro et al, 2020. Of these two modes, the most frequent is inflation, which typically occurs in flat areas (slopes <2°) (Bravo, 1964; Peterson et al., 1994; Pasquarè et al., 2008; Kempe, 2012). Inflation is associated with both pahoehoe and aa flows, and the magnitude of the inflation strongly depends on effusion rates (Calvari and Pinkerton, 1999; Jones et al. 2018; Kempe 2019).

Lava tubes are not only found on Earth. Indeed, analogous structures such as pit chains and skylights have been identified on surfaces of other rocky bodies of the Solar System, such as Mars and the Moon (Greeley, 1971a, 1973; Greeley and Spudis, 1981; Horz, 1985; Haruyama et al., 2009, 2012; Cushing, 2012; Sauro et al., 2020; Titus et al. 2021). Lava tubes on Earth and other planetary bodies differ in their size due to diverse effusion rates, sometimes as an effect of the different gravity (weaker gravity resulting in higher effusion rates). This difference leads to the formation of *pyroducts* (a synonym for *lava tubes*, a term introduced initially by Coan, 1844) which are smaller in diameter on Earth (10 - 30 m) than on Mars (250 - 400 m) and the Moon (500 - 1100 m) (Sauro et al., 2020). Despite this different scaling, the largest lava tubes on Earth are considered to be very useful analogues to their extra-terrestrial counterparts. In this regard, the La Corona lava tube in Lanzarote (Canary Islands) is of particular relevance, with a total length of about ~7.6 km (~9.7 km of total cave development) and a width reaching up to ~28 m for some of its sections (Bravo, 1964; Montoriol-Pous and De Mier, 1969; Carracedo et al., 2003; Sauro et al., 2019, 2020). It represents one of the largest pyroducts known on Earth, being comparable, in terms of volume, only to a few others such as the *Kazumura Cave* of Kilauea Volcano in Hawai'i (Allred and Allred, 1997; Kempe, 2012), the *Undara System* in Queensland (AUS) (Atkinson et al., 1975), the *Víðgelmir* and *Bùri* in Iceland (Wood, 1974; Water, 2006; Detay et al., 2011) and others in Arizona and Utah (Bunnell, 2013). The Ka Corona lava tube is one of the volcanic products of the *Canary Island Seamount Province* (CISP), a magmatic province that forms a disseminated hotspot track sitting atop old Atlantic Ocean seafloor (150-175 Ma, Roeser, 1982; Klitgord and Schouten, 1986; Roest et al., 1992; Figure 1), ~1300 km long and ~350 km wide, parallel to the north-western African continental margin (Hansen Machin and Pérez Torrado, 2005; Hoernle and Carracedo, 2009; van den Bogaard, 2013). Most of the CISP has been generated ~30 Ma, while the absolute motion of the African plate has been nearly stationary (ca. 8-10 mm/yr) (Silver et al., 1998; Carracedo et al., 2003; Gaina et al., 2013; van den Bogaard, 2013). This slow plate velocity makes this volcanic environment one of the best terrestrial analogues for the single-plate tectonics on Mars (Dañobeitia and Canales, 2000; Meyzen et al., 2015).

Within this context, our work aims to identify the processes that shaped the La Corona lava tube in order to understand the origin, evolution and degradation of this subterranean structure. In order to disentangle the processes, we have carried out a study of the satellite images of the northern region of Lanzarote, followed by field exploration of inner portions of the La Corona lava tube and adjacent areas. A laser scanner survey allowed us to proceed to the three-dimensional reconstruction of the main conduit portions. Sampling was carried out inside the pyroduct to characterize the geochemistry of the various lavas providing constraints on the timing of and genetic relationships between the different lava flows.

2 Geological overview

The Canarian archipelago comprises an elongated arcuate chain of seven major volcanic islands and numerous islets and seamounts located off the northwest coast of Africa (Hoernle and Carracedo, 2009, Figure 1). The origin of the island chain is thought to be hotspot-related (Morgan, 1983; Duncan, 1984; Ancochea et al., 1996; Carracedo, 1998; Dañobeitia and Canales, 2000). The hotspot track progressed towards the south-west, as shown by the irregular succession of decreasing island ages (Figure 1). The lack of a perfect age-distance correlation within hotspot-related archipelagos in slow-moving plates such as the Canary archipelago (Figure 1a) reflects the long-term spatial focussing of the volcanic activity within a restricted area (Meyzen et al., 2015).

2.1 Lanzarote

2.1.1 Geological setting of Lanzarote island

Lanzarote island is the north-eastern extension of the Fuerteventura-Lanzarote volcanic platform, as the sea depth in the narrow *La Bocaina* strait between the two islands does not exceed 40 m. Indeed, Lanzarote and Fuerteventura are the subaerial parts of a single volcano built along a possible fissure striking northeast-southwest parallel to the African coast. Lanzarote could be the longest-lived island of the archipelago, since the oldest subaerial volcanism is dated at ~15.5 Ma

(Figure 1b; Coello et al., 1992; Carracedo et al., 1998; van de Bogaard, 2013), while the last activity took place in 1824. It is old enough for erosion to have drastically smoothed its relief compared to other Canary Islands, reaching a mere 671 m at the highest point. Early submarine remnants of the shield building stage do not outcrop on Lanzarote (Hoernle and Carracedo, 2009). The oldest accessible massifs (Los Ajaches and Famara) are of Miocene age and represent late cycles of the shield stage (Hoernle and Carrecedo, 2009). *Los Ajaches Massif* was emplaced between ~15.5 and ~5.7 Ma in the southern part of the island (Hoernle and Carrecedo, 2009; Figure 1b), while a distinct magmatic event generated the *Famara Massif* between ~10.2 and ~6.3 Ma in the north-eastern part of the island (Abdel-Monem, Watkins and Gast, 1971; Coello et al., 1992; Carracedo et al., 2003; Hansen Machin and Pérez Torrado, 2005; Cabrera Vega, 2010; van den Bogaard, 2013; Figure 1b). Hiatus periods separating the three main different stages of Famara shield subaerial growth are marked by the presence of soils and calcretes deposits particularly well-developed at the top of each succession (Coello et al., 1992; Carracedo et al., 2003; Hansen Machin and Pérez Torrado, 2005; Cabrera Vega, 2010; Lomoschitz et al., 2016).

The more recent post-erosional stage took place in the Quaternary as a massive outpouring of fluid basalt, fed by a northeast-southwest alignment of volcanic vents, that flooded most of the surface of the island (Coello et al., 1992; Carracedo et al., 2003; Hansen Machin and Pérez Torrado, 2005; Cabrera Vega, 2010; van den Bogaard, 2013). In the north of Lanzarote (where our study area is located), this activity crowns the massif of Famara with the build-up of the volcanic system of La Quemada-La Corona-Los Helechos between ~91 to ~21 ka (Hansen Machin and Pérez Torrado, 2005; Hoernle and Carrecedo, 2009; Figure 1-2). The last volcanic phase corresponds to the *Historic eruptions* occurring in the central region of the island in 1730-1736 and 1824 (Hoernle and Carrecedo, 2009; Gómez-Ulla et al., 2018; Figure 1b).

2.1.2 La Corona Volcano

La Corona volcano is one of the edifices of the La Quemada-La Corona-Los Helechos volcanic alignment (Figure 1b, 2e). Although these edifices were thought to be derived from a single eruption for many years (Luis and Quirante, 1984), Los Helechos and La Quemada emplaced around ~91 ka, while La Corona erupted later during the Last Glacial Maximum (LGM) around ~21.6 ka (Figure 2b; Carracedo et al., 2003; Hansen Machin and Pérez Torrado, 2005).

The higher (than Canary average) dimensions of La Corona volcano [cone width (W_{co}) = 1.500 m; crater width (W_{cr})= 500 m; cone height (H_{co}) = 269 m] can only be generated by voluminous eruptions and high effusive rates (Carracedo et al., 2003). Over its eastern flank, adjacent to its main crater, a secondary crater is visible within a 200 m wide channel-like depression terminating in a potential sinkhole at the bottom of the volcanic edifice (Figure 3). A similar process occurred at Fagradalsfjall (Geldingadalir) Volcano in Iceland during an eruption in June, 2021 (see video, from 01:16).

The edifice construction of La Corona (Figure 2c) happened into two main phases: 1) an initial Strombolian episode during which the volcanic cone built up, and lapilli deposits were radially spread in a wide area around the main vent and 2) a second phase dominated by effusive lava emission. The cone morphology suggests a moderate intensity of Strombolian explosions with a greater accumulation of pyroclasts close to the eruptive centre forming the steep slopes (28-30 degrees) of the volcanic edifice (Bravo, 1964; Carracedo et al., 2003). The subsequent effusive phase can be subdivided into two different episodes of lava emission. The first event (from here onwards C1) was characterized by huge volumes of basaltic pahoehoe-type lava, that flowed down the eastern slope burying the pyroclastic material of the Strombolian phase and the previous La Quemada-Los Helechos lava flows (~91 ka, Carracedo et al., 2003). This massive discharge of lava enlarged the areal extent of the island toward the northeast by ~100 m beyond the former coastline (Hansen Machin and Pérez Torrado, 2005) (Figure 2e). Subsequently, a second effusive episode releasing a greater volume of viscous lavas of predominant aa-type (Figure 2d) took place (from here onward C2). C2 only partially covered the lava field previously created by C1 (Figure 2e). These two main effusive events produced a broad fan-shaped basaltic plateau of ~18 km^2, called by the local s the *Malpaìs de La Corona*. The lava tube, digging the south eastern side of the volcano, is of uncertain attribution, and may have been formed during any of the emission episodes of C1 and C2.

2.1.3 La Corona lava tube system

The La Corona lava tube originates from a sinkhole, located at the base of the south-eastern side of La Corona volcano and heads from there towards the coast with a northwest-southeast direction (Figure 3). It has a length (L_t) of ~7.6 km (of which ~6.0 km are subaerial and ~1.6 km submerged), with a total extension to ~9.7 km when side branches and upper levels are considered. The conduit has a mean width (W_t) of ~13.7 m and average height of ~10 m and a total difference in topographical elevation of ~374 m (~310 m above current sea level and ~64 m below it) (Sauro et al., 2020).

The tunnel's sinuous path can be easily tracked owing to the numerous *skylights* and collapses (*Jameos* in the local dialect and *Pukas* in Hawaiian) forming a northwest to southeast chain recognizable both from the surface and aerial views (Figure 3).

The La Corona lava tube is not walkable for its entire length; numerous collapses obstruct the cave passages in the upper part. Each of the major Jameos networks (Jameos de los Molinos, Jameos de Arriba and Jameo de Francisco Leòn, Figure 3) in the vicinity of the La Corona crater (< 1 km) located on the plateau of Famara massif (> 250 m) prevents humans from accessing the interconnections between sections. The last ~1.7 km of the tube are submerged below sea level, because of the marine transgression that occurred after the LGM (~21 ka; Labeyrie et al., 1987; Bard et al., 1990). The most accessible and walkable portions of the tube are stretched over six sections (Figure 3): I) Jameo de los Prendes – Jameo de la Gente (~1170 m); II) Jameo de la Gente – Jameo de la Puerta Falsa (~1165 m); III) Jameo de la Puerta Falsa – Jameo de los Verdes (~1290 m) and IV) Jameo de los Lagos/Perdido (~730 m); V) los Jameos del Agua (~350 m); VI) Tùnel de la Atlantìda (Montoriol-Pous and De Mier, 1969; Isler, 1989; Mendo and Ortega, 1988; Carracedo et al., 2003; Smith, 2010; Sauro et al., 2019; Figure 4).

In some places, the tube has developed a multi-level architecture. Superposed levels can be formed by two (not mutually exclusive) processes: i) smaller branches reconnect with a principal one beneath (Bravo, 1964), ii) a smaller lava tube forms at the base of a partially drained larger tube (multi-levels/tube-in-tube structure; Bunnell, 2013; Shick, 2017). The latter mechanism is visible in several places, in particular along the la Gente – la Puerta Falsa stretch, where an upper conduit runs below Jameo Tacho, Jameo Cumplido and Jameo Agujerado, and is not reachable from the tube-in-tube structure beneath (Figure 5d).

From Cueva de los Lagos toward the coast, due to its lower elevation, the tube becomes exposed to marine ingression and thereby to tidal changes of the water level. The final submerged segment of the lava tube, called *Tùnel de la Atlantìda* (Isler, 1989; Mendo and Ortega, 1988; Carracedo et al., 2003) starts from Jameos del Agua (nowadays a tourist site, Figure 3m, and 7) and continues for over ~1.6 km under the ocean, reaching a depth of -64 m ca. below sea level, where the tube ends abruptly, forming a large spherical cavity (10x10 m) (Chappell and Shackleton, 1986;

Carracedo et al., 2003). There are no discernible signs of magma-seawater interactions along most of the tube extension (~7.6 km). This suggests that, at the time of the eruption and therefore of the emplacement of the lava tube, the sea was in a phase of regression and the coastline was about 80-120 m lower than today. Thus, the eruption took place while the marine platform was a dry land (Carracedo et al., 2003; Sauro et al., 2019). This emplacement framework is coherent with the paleoclimatic data collected by Labeyrie et al., (1987), that places the sea level variation between 18 - 21 ka, during the LGM event.

3. Materials and Methods

3.1 Geological mapping

A new geological map at a scale of 1:25,000 m for a wide area covering approximatively 70 km^2 in the north-eastern part of Lanzarote was created using high-resolution images (DTM 5 m from the Lidar topography provided by the *Spanish Geological Service*) and field survey observations (Figure 2e). The field work has been carried out both at the surface and inside the lava tube.

One of our primary goals was to first check geological boundaries deduced from preliminary interpretations of remotely sensed imagery. Photogrammetric acquisitions with Unmanned Air Vehicles (UAVs) at the surface and laser scanning surveys within the tube were also performed during the field campaign. The UAV surveys were constrained by GPS points within the tube collapses themselves and at their edges; these edge points were used to constrain the underground LiDAR data to the surface by point-cloud co-registration. This procedure allowed integration of the tube into a geographic-projected reference system and correlation of the contacts between units within the tube, with those observed and mapped at the surface.

3.2 Laser scanning

Terrestrial Laser Scanning (TLS or T-LiDAR) technology was employed to reconstruct the three-dimensional model of the volcanic cave system, using two different devices: a Leica HDS 7000 laser scan mounted on a tripod and a wearable Leica Pegasus Backpack for acquisition during motion within the cave.

During the acquisition phase the Leica HDS 7000 instrument recorded 1,016,727 pts/sec, with a maximum range of 187 m. Since the Leica HDS 7000 is a rather heavy and delicate instrument, for some of the more difficult to explore portion of the tube , we used the Leica Pegasus Backpack, which is more manageable (~12 kg weight), easily wearable, and optimised for indoor data capture. In this case the instrument recorded 600,000 pts/sec, at a maximum range of 50 m.

We performed a total of 440 scans, to map ~5.6 km of cave passages, including the different sections connected to each other through the sinkholes. The main part of the tube system, from Jameo de los Prendes to Cueva de los Verdes (Plate 3 in Supporting Information S1), was mapped with a resolution of 0.25 m. To be able to georeference the point clouds, without any GPS information (since the survey was conducted underground), the point clouds representing various tube sections have been mutually co-registered, initially with the UAVs photogrammetric surveys and then integrated to the LiDAR topography of Canary Island (gridded at 5.0 m). The analysis and treatment of LiDAR data were carried out using CloudCompare (CC) software and the Python programming language. Working on point cloud clusters enabled us to obtain both perpendicular and transverse sections of the lava tube (Supporting Information S1). In addition, the three-dimensional reconstruction of the tube allowed the recognition of several internal morphologies such as *flow ledges* (or benches, Figure 5a), *cupolas* (dome-like heightening in a lava tube's ceiling, Figure 4b) and *windows* (openings between different levels, Figure 4c) as catalogued in Bunnell (2013).

3.3 Sample selection, location and analytical procedure

3.3.1 Magmatic rocks

The sampling strategy was primarily aimed at collecting the whole spectrum of lithological units intersected by the lava tube along most of its length. We will refer to these units as *pre-existing lava flows*. These samples were collected above or below a recurrent red pyroclastic layer at three cross-sections, located at distances of approximately ~1.5 km (SUB1), ~2.3 km (PL1, PC1) and ~2.6 km (LPUB1, LPLB1, LPCV1) from the sink as shown in Figures 2 and 6 a-c. The second goal was to sample the "cave material" (PC1 and LPCV1, Figure 6 a-c), namely the inner flows of the tube (e.g. floor deposits, lining walls, etc.). A sample (CRB1) from the upper Famara unit was also collected to allow a geochemical comparison with samples from the tube (Figure 2). Samples were sorted with respect to phenocryst abundance, mineralogical assemblage, vesicularity and extent of alteration. After this categorization, major and trace element analyses were performed on seven samples (Table 1). A brief description of their petrography is given in Supporting Information S2. Major and trace element contents were measured at the *Service d'Analyses des*

Roches et des Mineraux (SARM-CNRS) at the *Centre de Recherches Pétrographiques et Géochimiques* (CRPG, Nancy, France) by Inductively Coupled Plasma Mass Spectrometry (ICP-MS) and Inductively Coupled Plasma Atomic Emission Spectrometry (ICP-AES) (Table 1). Analytical errors are less than 2% for SiO_2, Al_2O_3, Fe_2O_3, MgO and CaO, and 5-15% for Na_2O, TiO_2, MnO, P_2O_5 and K_2O. Long-term precision (% RSD) for the procedure is typically better than 15% for trace elements and 5-10 % for Rare Earth Elements (REE).

4. Results

4.1 Subsurface morphologies

The massif of Famara in the northern part of Lanzarote is made up of at least three different volcanic stages interlayered by erosive discordant surfaces, sedimentary deposits and soils (Dóniz Páez et al., 2002; Meco et al., 2003; Hansen Machin and Pérez Torrado, 2005), and is overlapped by the Quaternary volcanic group of La Quemada-La Corona-Los Helechos (Figure 1b, 2e).

The La Quemada lava flows stretch from the volcanic cone of La Quemada (de Orzola) through the north-eastern side of Famara massif to reach as far asthe northern coast of Orzola (Figure 2e). The Los Helechos volcanic sequence begins with pyroclastic deposits (outcropping inside the quarry of Maguez and along the sides of the *Mesa de Los Llanos* nearby) followed by widespread lava flows emitted from the vent alignments of Los Helechos which is formed from north-east to south-west by La Cerca, El Helecho and La Quemada de Maguez vents (Figure 2e). Los Helechos lavas cover a wide area that - from the volcanic cones in the Maguez district - reach the eastern coast at the villages of Arrieta and Punta Mujeres (Figure 2e). A small lava flow on the western side of the Los Helechos volcanic edifice crosses the physical boundary constituted by the Famara cliff to reach the western coast (Figure 2e).

La Quemada and Los Helechos lava fields were covered by the effusive events of La Corona, creating a new fan-shaped area that extended beyond the current coastline (Carracedo et al. (2003); Hansen Machin and Pérez Torrado, 2005). While entrenching the south-eastern slopes of La Corona volcano, the lava tube system of La Corona may have intersected to some extent the lava fields generated by the La Quemada-La Corona-Los Helechos alignment (Figure 2e). At the entrance to collapses, the pre-existing lava succession has been clearly cross-cut by repeated injections of molten lava flows. This constitutes an unquestionable indication of an *inflation-type* formation process (sensu Kempe, 2012).

The huge amount of debris inside both the collapses and the conduit indicate *breakdowns* (collapses of ceiling and lining walls; Bunnell, 2013), which occurred mainly during and after the cooling phase of the lava tube itself. Often, the conduit walls are covered by a coating of thin layers of lava (*lining walls* in Harter, 1972; Bunnell, 2013; or *glaze* in Shick, 2017) accreted onto the underlying coarser basalts during the passage of the molten lava flows. Once the first layer has formed, repeated temporal fluctuations in lava height and hence in the volume rate of flow can deposit additional layers, glazing the tube walls, and covering up the pre-existing lava flows. If the stream-flow rate remains stable, deposits on the walls will grow into flow ledges. Flow ledges are terrace-shaped lava accumulations, preferentially formed at the external wall of meandering lava tubes (Figure 5a). Morphologies such as flow ledges grow by overbank events involving thin lava layers (Kempe, 2012). In the case of prolonged and gradual decreases of flow rates, the flow ledges might grow up as a “secondary ceiling” above the flowing lava, forming a tube-in-tube structure (Figure 5d; Kempe, 2012 and Shick, 2017, for similar examples in Hawaii). This process can be recognized by the presence of multiple levels of tubes that run in parallel, one above the other, often vertically connected through cavities called windows (Figure 5c).

The La Corona lava tube shows a single-type large tunnel structure, evolving towards a multi-level architecture in some sections. From Jameo de los Prendes to Jameo Tacho it has a single section (15-20 m wide, Plate2 in Supporting Information S1), while from Jameo Tacho to Jameo de la Puerta Falsa the section is divided into two conduits (4-5 m wide, Plate2 in Supporting Information S1) and, in some sporadic segments, into three conduits (3-4 m wide, Figure 5c and Plate3 in Supporting Information S1). In this particular section, the upper conduits are not fully accessible because of collapses that obstruct their entry points, while the lower conduit runs undisturbed until Jameo de Puerta Falsa. Some sections between Jameo de la Puerta Falsa and Jameo de los Verdes are similarly divided into two superimposed conduits (5-10 m wide, Plate3 in Supporting Information S1). At Cueva de los Verdes, the different conduits merge into a single large tube, reaching a maximum height of 37 m, often divided into two to three levels separated by secondary ceilings. In Jameo de los Verdes, the tube is interrupted by a breakdown, but can be accessed again at Jameo de los Lagos (Figure 3). From there, the tube mainly continues as a single conduit up to the seven underground lagoons (from which the cave takes its name). Recently it was discovered that on top of the second underground lake a second superimposed conduit develops for 70 m with heights of up to 15 m. From Cueva de los Lagosit was originally possible to reach the cave complex of Jameos del Agua, where progress is blocked by tourism infrastructure. Then, from Jameos del Agua, the tube “sinks” under the present-day sea level for 1.6 km as the Tùnel de la Atlantìda. The tube is also characterized by the presence of knickpoints in the floor level, that facilitate the downcutting processes (Allred and Allred, 1997; Kauahikaua et al., 1998; Keszthelyi and Self, 1998 and Kempe, 2012; for similar examples in Hawaii). The most evident knickpoint is the one that marks the topographic step between Famara massif and La Corona lava field plane (Malpaìs de La Corona). Other knickpoints were identified by the three-dimensional model of the tube. They are probably related to sharp changes in the paleo-topography reflected in the tube channel slope. In association with knickpoints or enhanced tube curvatures, cupolas can develop in the tube ceiling. They form where lava under pressure caused melting upwards into a hardened ceiling (Figure 5b). Under sustained flow, the cupola formation process might breach the ceiling creating a window, toward an eventual upper tube (Figure 5c), or even a skylight. Lower levels, representing the last active part of the tube, may overflow into upper levels through windows, leaving deposits along the flow ledges that can grow and eventually seal the windows (Figure 5d).

4.2 Linings and entrenched units

Lining wall breakdowns are more frequent in the initial part of the tube, exposing pre-existing lava flow sequences cross-cut by the tube emplacement. A reddish deposit of lapilli in an interlayered position in the lava flow pile is conspicuous when examining pre-existing lava flows sections (Figure 6). This pyroclastic deposit has a variable thickness, ranging from 40 cm to 1 m. The pyroclastic level is composed by layered pyroclastic fallout deposits, that do not show any cross stratifications or other evidence of pyroclastic surges or pyroclastic flow arrangement (Figure 6). The sequence is characterised by parallel layers of pyroclasts sorted by size ranging from mm to cm scales. Very similar in aspect to the dark pyroclastic material that covers the La Corona volcano sides, the red layer appears repeatedly in most segments of the tube, if not hidden by lining walls (Figure 6). For these reasons, we consider it to be a reference stratigraphic level. The reddish colour of the lapilli layer is due to oxidation driven by the presence of water vapour and oxygen within the lapilli intergranular porosity at high temperature during the flow of molten lavas within the tube (Waters et al. 1990; and see Shick, 2017 for similar examples in Hawaii).

Lava sheets under and above this reference level show clear differences in morphology, thickness, phenocryst content and alteration state. The lava flows underneath the pyroclastic level (from here onwards termed *lower units*) are more massive and thicker (60-140 cm) than the much porous upper flows (from here onwards termed *upper units*). They are also more altered and fractured and show "onion skin" shells typical of spheroidal weathering (e.g. Ollier, 1971; Chatterjee and Raymahashay, 2015), indicating rock-water interaction before the emplacement of the pyroclastic layers. However, the absence of any trace of soils and/or calcretes – which are typical of the Famara complex – suggests that these flows must be largely subsequent to the Mio-Pliocenic Famara event. The upper, pre-existing, lava flows have instead a moderate individual thickness (40-80 cm), an aphyric texture and do not show any evidence of spheroidal weathering, indicating a limited duration of exposure to exogenous agents. However, they are less massive and present a higher degree of vesicularity (avg. 6% for lava flows' cores in the upper unit vs less than 1% for cores in the lower units, see Supporting Information S2). Neither of the basaltic successions (lower and upper units) show any signs of interaction with seawater during the active stream-flowing of molten lava.

4.3 Paleo-topography derived from three-dimensional reconstruction

As previously described in section 2.1.1, the La Corona eruption began with Strombolian explosions, that spread a layer of pyroclastic material over a wide area surrounding the volcanic edifice. This blanket of lapilli was then successively covered by effusive lava flows from both first (C1), and second (C2) major phases. The external deposits of dark lapilli were mapped by remote sensing and field surveys (Figure 2e), while the positions of the lapilli deposits within the tube have been reported inside the reconstructed three-dimensional internal tube morphology retrieved by TLS. Since GPS measurements are not possible underground, the lapilli layer locations within the tube were retrieved using the distances from the Jameos entrances, relative height of the lapilli deposit within the tube, photos and campaign notes. In this way, the inner path of the lapilli layer is constrained in relation to both its underground exposures within the tube and outcropping deposits at the surface, as displayed in the geological map (Figure 2e).

Using ArcGis – Kriging Tool and Cloud Compare software programs, we were able to generate a mesh surface which, to a good approximation, represents the paleo-topography covered by the layer of lapilli of the Strombolian event. This surface was obtained by the interpolation of the red lapilli layer within the tube and the dark lapilli deposits outcropping at the surface. As expected, the *reconstructed* paleo-topography is rather smooth and gentle, similar to the current one. The presence of such flat paleo-relief might be related to the very long hiatus between the eruptions of the last Miocene and early Pleistocene units, which would have enabled erosion to drastically reduce most of the pre-Pleistocene island relief. In addition, the reconstructed surface (Figure 7), highlights how the pyroclastic horizon runs along almost the entire lava tube (see Supporting Information S1).

Other detailed observations are:

- Approximately 30-40 m upstream from the collapse of Jameo de los Prendes, the red layer is visible at the top of the tube vault, before being buried behind the lining walls (sections 1.01 in Plate1, Supporting Information S1) and reappears at floor level next to the Jameo entrance (Figure 6a; sections 1.03 in Plate 1, Supporting Information S1).
- In the upstream branch of Jameo de la Gente, the red layer roughly crosscuts the upper height of the tube (Figure 6b; Plate 1 in Supporting Information S1).
- From Jameo de la Gente to Jameo de la Puerta Falsa (Figure 6c; Plate2 in Supporting Information S 1), the reconstructed layer is often covered by the lining walls, but on some occasions, reddish lapilli are visible right under aligned flow ledges.
- Downstream, in the section from Jameo de la Puerta Falsa to Jameo de los Verdes (Plate3 in Supporting Information S1), where the tube divides into a tube-in-tube structure, the reconstructed layer lies at the top of the lower tube. Indeed, pockets of reddish lapilli appear under the flow ledges responsible for the tube-in-tube structure.
- In Jameos del Agua, the layer of reddish lapilli lies in the lower half of the main conduit, forming a more hollowed side ledge (which was largerly covered by concrete consolidation during the adaptation of the site for tourism).

Therefore, it is certain that the reddish lapilli layer is present along the whole terrestrial part of the tube development. In cross-sections, it can be found at the ceiling, close to the ceiling, in the middle or lower part, but never at the lower floor level.

4.4 Geochemical results

We document here geochemical variations for aphyric samples from the tube linings and the pre-existing lava flows cross-cut by the tube. Their variations are compared with earlier data, acquired from the same units retrieved from GEOROC, during previous studies (Ibarrola and Lopez, 1967; Santin, 1969; Ibarrola, 1970; Thomas et al., 1999; Carracedo et al., 2003; Lundstrom et al., 2003).

Our goal is to identify any significant chemical compositional differences between pre-existing units that could help us to pin-point the nature of the units intersected by the lava tube underground.

4.4.1 Chemistry of Quaternary volcanism compared to the Mio-Pliocene Famara complex

The Mio-Pliocenic samples of the Famara complex, CRB1 and literature data (Ibarrola and Lopez, 1967; Santin, 1969; Ibarrola, 1970; Thomas et al., 1999; Carracedo et al., 2003; Lundstrom et al., 2003), were used as a benchmarks to compare our samples with those relating to Quaternary volcanism (Figure 8). When major element chemistry is considered in relation to MgO (Figure 8), the Famara field is indeed well distinguishable from those related to the Quaternary volcanism. In particular, progressively from the Mio-Pliocene samples to the Quaternary samples there is a tendency for the proportion of SiO_2 to increase, while CaO, and to a lesser extent FeO^T and TiO_2, decrease (Figure 8).

The composition of all our samples taken from the units above the pyroclastic level (upper units) fit with the composition of the Quaternary volcanism reported in the literature (Los Helechos, La Quemada, La Corona) and fall outside the values obtained from the Famara field, with the only exception being the Na_2O-MgO content. The lining wall samples (PC1, LPCV1) are in contrast compositionally different from the homologous ones reported in literature, but still clearly distinguishable from la Famara field.

The samples taken from beneath the pyroclastic horizon (lower units' samples, PL1 and LPLB1) are the only ones that systematically overlap with the Famara field (Figure 8). Nonetheless, their potential association with the Famara series is ruled out by trace element analysis (Figure 9). The Famara spiderdiagram is distinct from those of all the other units (above and beneath the pyroclastic horizons as well as the lining walls) because of its characteristic positive slope in the trend from Ba to Ta and the noticeable absence of a pronounced negative anomaly in Zr-Hf (Figure 9).

4.4.2 Major element chemistry of the Quaternary volcanism

In a total alkali (Na_2O+K_2O) versus silica (TAS) diagram (Figure 10), there is a clear systematic difference in the nature of lavas located below and above the lapilli reference layer. Pre-existing lavas underneath the lapilli layer (PL1 and LPLB1) are classified as basanites. LPLB1, a sample from the lower units, is the most alkali-enriched sample of this group, overlapping with previous data published for Los Helechos (Carracedo et al., 2003; Lundstrom et al., 2003) and La Quemada (Ibarrola and Lopez, 1967; Carracedo et al., 2003; Figure 10). In contrast, wall lining deposits (PC1, LPCV1) and lava flows (SUB1, LPUB1) located above the reference layer systematically fall in or near the basaltic field (Figure 10), defined by earlier published data for La Corona samples (Ibarrola and Lopez, 1967; Thomas et al., 1999; Carracedo et al., 2003; Lundstrom et al., 2003). Another systematic difference between compositions of the samples from the upper andthe lower units is the MgO range (Figure 8). MgO among the lower units samples (PL1 and LPLB1) has a 12.8-12.2 % range, with a mean of 12.5 %, substantially higher than the 11.5-9.1 % range 10.3 % and mean of of the upper units (SUB1 and LPUB1) and the 7.4-9.4 % range, and 8.4 % mean, of the lining wall (LPCV1 and PC1) samples. Note that the lining wall samples are among the most differentiated samples of our dataset.

When major element chemistry is considered in relation to MgO, other geochemical differences become even clearer. Samples from lower units (PL1 and LPLB1) display higher FeO^T and lower SiO_2 and Al_2O_3 content than those of the upper units (SUB1 and LPUB1) and lining walls (LPCV1 and PC1). In detail, the lower unit sample LPLB1 lies within or closely adjacent to the field defined by previously published Los Helechos data (Carracedo et al., 2003; Lundstrom et al., 2003), while sample PL1 shows no overlap (Figure 8). The high TiO_2 values place the lower units samples above those of both the La Quemada (Ibarrola and Lopez, 1967; Carracedo et al., 2003) and La Corona compositional fields, (Ibarrola and Lopez, 1967; Thomas et al., 1999; Carracedo et al., 2003; Lundstrom et al., 2003) and they fall in the range of samples identified as from Los Helechos but with slightly higher MgO contents (Carracedo et al., 2003; Lundstrom et al., 2003). As expected, samples from the upper units (SUB1 and LPUB1) fall or plot closely adjacent to the field defined by earlier data for La Corona units (Ibarrola and Lopez, 1967; Thomas et al., 1999; Carracedo et al., 2003; Lundstrom et al., 2003; Figure 8). The composition of our lining wall samples (LPCV1 and PC1) is enriched in Na_2O and TiO_2 compared to the upper units (SUB1 and LPUB1) (Figure 8). However, as already noted, they are remarkably compositionally unlike the previous lining samples published by Carracedo et al., (2003), even if their trace element patterns are closer to those of La Corona rather than Los Helechos. The differences with previous data published on other lining samples might potential be due to different degrees of contamination while the lava was flowing within the tunnel due to thermal erosion of pre-existing lava flows.

4.4.3 Trace element chemistry of the Quaternary volcanism

Primitive-mantle-normalized incompatible element patterns for our samples (Figure 9) reveal subtle compositional differences between upper and lower units. While samples from lower units (PL1, LPLB1) have subparallel spiderdiagrams with an extremely restricted range of concentrations, the same is not true for samples from the upper units (SUB1, LPUB1). The latter exhibit two distinct spiderdiagrams, with greater enrichment in highly versus moderately incompatible trace elements for sample SUB1 relative to sample LPUB1 (Figure 9). Although spiderdiagrams of the lower unit samples (PL1, LPLB1) overlap with that of sample SUB1, a detailed examination shows a distinct fractionation in Th-U relative to Nb and a more pronounced negative Zr-Hf anomaly for SUB1 relative to samples from the lower units. If LPUB1 is also considered, it becomes clear that the steeper fractionation of Th-U relative to Nb is a general feature of the upper units relative to lower ones (Figure 9). The spiderdiagrams of the lining wall samples display a slightly lower fractionation of highly to moderately incompatible elements than SUB1 and samples from the lower units, although their overall patterns share more similarity with sample SUB1.

5. Discussion

5.1 Geochemical constraints on the units crossed by the La Corona lava tube

There is a great compositional difference in terms of major elements between the upper and lower units enclosing the pyroclastic layer (Figure 8). Although samples from the lower unit, (PL1) do not complitely overlap with the field defined by the literature data (Ibarrola, 1970; Carracedo et al., 2003; Lundstrom et al., 2003) for the massif of Los Helechos, they represent an extension of major elements trends defined from published Los Helechos lava analyses to substantially higher MgO values (Figure 8). The other sample from the lower units (LPLB1) systematically falls within the Los Helechos field. We therefore, conclude that basanites (PL1 and LPLB1) from the lower units compositionally resemble samples from the Los Helechos sequence, confirming that the lava tube entrenched the pre-existing unit at its base. The lining sample (LPVC1) is also of clear La Corona affinity, while the other lining sample (PC1) is the most differentiated one falling in the extension of major elements trends established by previously published data for La Corona. Their primitive-mantle-normalized incompatible element patterns closely resemble that of sample

(SUB1) from to the upper lava flow and which is interpreted to be an expression of the La Corona C1 magmatic event.

5.2 Lava tube genetic mechanism and morphologies

The structural and geological study conduited on the northern region of Lanzarote and in particular the field observation of the La Corona lava tube system coupled with the geochemical analyses raised the following considerations:

1. the pyroclastic deposits at the surface mark the first Strombolian event of La Corona, which covered the Los Helechos sequences;
2. the pyroclastic layer inside the tube can be correlated with early La Corona pyroclastic deposits onto at the surface, allowing the definition of a reliable paleo-topography at the time of the La Corona Strombolian event and before the C1 first stage of lava emplacements;
3. the spatial positioning of the lapilli surface within the three-dimensional tube reconstruction shows (Figure 7) how the lapilli layer characterizes the pyroduct through the entire length of the tube.

All these points suggest that the lapilli deposit in-between the Los Helechos and La Corona lava flows, may have greatly facilitated the early inflation process of the La Corona tube system, as reported for other lava tubes in Hawaii (Greeley et al., 1998). With regard to the early stages of its development, our data suggest that the lava tube emplacement happened after the pyroclastic deposit and during the effusive stage of the La Corona event. In particular from field and geophysical data (Torrese et al., 2021), it is evident that the tube was excavated underneath 10 to 20 m of lava flows and was well-developed within ~900 m from the main vent. Since the pyroclastic horizon is visible at 15 m of depth at Jameo de los Prendes (~1 km down from the first Jameo de los Molinos, Figures 3b and 6a, and section 1.03 in Plate1, Supporting Information S1) and in view of its regional position and dip (Figure 7), it is very likely that the same layer is at a similar depth upslope, although in that case overlying the Famara massive. This implies that the tube was already progressing within the pyroclastic deposits just 20 m from the putative sinkhole at the base of La Corona volcano (Figure 3).

We therefore envisage that the general process of initial inflation would have begun as the effusion rate increased and the lava stream flooded laterally from the primary and secondary vents. The steep slope gradient promoted the thermomechanical excavation at the base of the volcanic edifice where the remnant of a potential sinkhole is visible (Figure 3, and 12). Such a process has indeed been reported by several authors as a viable mechanism for forming a *sink pond* (or plunge pool, sensu Allred and Allred, 1997; Kempe, 1997; Greeley et al., 1998; Keszthelyi and Self 1998; Smith et al., 1998; Kauahikaua et al., 1998; Bunnell, 2013). It is very likely that the initial tube formation began with the deepening of the sink pond. The hot lava made its way through lava sheets stack inflation and downward thermal erosion through the pre-existing lava flows down to the level of pyroclastic layer, which was reached within a distance of 250 meters from the sink. This suggests that the inflation between lava flows, as defined by earlier studies (Hon et al., 1994; Kempe, 1997; Greeley et al., 1998; Kauahikaua et al., 1998; Keszthelyi and Self, 1998), took place during a very early phase and mainly in proximity of the volcanic edifice. Then, most of the flow was afterwards injected between the pyroclastic layer and the previously emplaced La Corona unit (C1). The repeated inflation of molten lava below not long before emplaced the C1 flows, allowed narrow streams to gradually incise the buried and unconsolidated pyroclastic layer (Figure 11), forming a series of tiny flattened elliptical ducts parallel to each other. Eventually one of these tubelets become dominant, while others stagnated. Once the lava flow reached the topographic step between the Famara massif and the current La Corona lava field overlying the former Los Helechos unit, it formed a lava fall. There the lava flow over-excavated deeper into the pre-existing lava field, reaching the pyroclastic layer interbedded between the C1 and Los Helechos flows. The general process would be similar to that described by Kauahikaua et al., (1998) in Hawaii, where the lava advanced as a complex, anastomosing system of small tubes.

This is confirmed by recent Electrical Resistivity Tomography (ERT) surveys orthogonal to the tube in Torrese et al., 2021. The identified series of elliptically-shaped channels have a width ranging from 7 to 13 m with a ceiling depth from the surface of 14 to 29 m. Most of them appear to be presently isolated from the main tube and were partially undrained and therfore short-lived features. A minor proportion remained active and experienced widening by lateral thermo-mechanical erosion of the weak pyroclastic layer by persisting stream-flows of molten lava. This is in full agreement with the theoretical and experimental treatment of thermal-erosion by Jarvis, (1995) and Kerr et al., (2001). The enlarged tunnel could have then grown by capturing nearby conduits, especially when the lava started to entrench down through thermal erosion, forming a much larger tube. The inflation directions of the lateral spreading were governed by topographical variations (i.e. slopes) and temporal and spatial variations in the volume rate of flow alternatively favouring different branches then conveyed to the main tube, as a result of consecutive downward erosion (Kempe, 2019). Once the pyroclastic layer was consumed, the new main tube continued its expansion through thermo-mechanical erosion by complete or partial melting and assimilation of the pre-existing substrate constituted by the upper and lower units as proposed in the pioneering work in Lanzarote by Bravo, (1964); in the Hawaiian context by Kempe et al., (2010), and Bauer et al., (2013) and in a komatiitic lava context by Williams et al., (2001, 2004, 2011).

Bearing in mind the morphological differences between upper and lower units (see section 4.1), we suppose that the enlargement mechanisms may have worked differently in the erosion of the different units. The less massive and more vesicular nature (avg. 6%) of the upper units made them more easily subject to mechanical erosion processes, in particular during sustained flow events where the conduits were under pressure flow conditions. While the low topographic gradients (slopes of ca. 2-3°) which characterise the north-eastern region of the island both nowadays and in the past contributed to reducing the flow rate, favouring a prolonged thermal contact between the overriding molten lava flow and the cold basaltic substrate of the lower units beneath. The transfer of heat into the substrate further reduces the hardness of the material already reduced by weathering, which would have encouraged its partial melting with consequent pyroduct downcutting below the pyroclastic layer (Bravo, 1964; Kauahikaua et al., 1998; Keszthelyi and Self, 1998; Williams et al., 2001, 2004, 2011; Shick, 2017). This long-lasting contact between hot and cold magmatic material together with the local turbulence of the flow induced by topographic irregularities of the tube floor and walls, would have promoted a combined effect of thermal and mechanical erosion of the pre-existing lava sheets (Jarvis, 1995; Greeley et al., 1998; Williams et al., 2001, 2004, 2011).

The downcutting along the La Corona lava tube increases downstream. In section II (Jameo de la Gente – Puerta Falsa; Figure 3 and Plate2 in Supporting Information S1), the tube has a maximum of two superposed levels, and its total height does not exceed 20 m, whereas in section III (Jameo de la Puerta Falsa – Jameo de los Verdes; Figure 3 and Plate3 in Supporting Information S1), the tunnel is entrenched in the form of a canyon with depths reaching up to ~40 m, and is composed of up to three superposed levels.Proceeding downstream the red pyroclastic layer is exposed at increasingly high levels on the tube walls with respect to its floor. The entrenchment progression was probably controlled by a process of knickpoint retreat in a similar process to what happens in river beds, and already proposed by Greeley et al., (1998), Kauahikaua et al., (1998), Keszthelyi and Self, (1998) and Kempe, (2012) for other lava tube systems. During the progressive drainage of the enlarged pyroduct, the flow activity was confined to the base of the cave. Consequently, the flow ledge accretion can lead to the formation of a second ceiling, isolating the lava flow to the inferior sector of the canyon and giving rise to the multi-level structure (e.g. Shick, 2017) clearly visible in section II (Jameo de la Gente – Puerta Falsa) and section III (Jameo de la Puerta Falsa – Jameo de los Verdes).

The combination of these processes has likely allowed the La Corona system to reach the considerable dimensions and the multi-level structure that it has today.

6. Conclusions

The genetic processes that led to the formation of the La Corona lava tube system were mainly driven by an initial inflation process and the subsequent capture of different flows along a main drainage conduit. A lapilli layer occurring at the earliest stage of La Corona volcanic activity seems to play a pivotal role in the establishment of an efficient draining tube system. This layer outcrops in several locations at the surface as a widespread deposit of dark lapilli, frequently visible within the tube as a reddish pyroclastic horizon where the breakdown of the lining walls exposes the pre-existing flows.

The three-dimensional reconstruction of the surface covered by lapilli shows that thelapilli run along almost the entire length of the pyroduct. This leads us to suppose that the incoherent lapilli horizon has favoured the excavation process of the molten lava, which in exploiting this weakness began to establish the lava tunnel itself (Figure 11). In particular surface observations have shown that the inflationary process began at a sinkhole conveying lavas at the base of the main edifice. Whitin a few hundred meters of the sinkhole, the underground hot lava was able to reach the pyroclastic layer underneath the pre-existing lava flows, allowing the tube system to be formed (Figure 12). The stream of lava ends up coalescing into a single large tube, as a result of consecutive downward erosion and the capture of nearby tubelets.

Geochemical analyses performed on aphyric basaltic flows from above and below the lapilli layer show that the lower units are of Los Helechos affinity, while the upper units are compositionally similar to La Corona flows. The samples were collected at distances of approximately ~1.5 km (SUB1), ~2.3 km (PL1, PC1) and ~2.6 km (LPUB1, LPLB1, LPCV1) from the sinkhole (Figure 2 and 6). Hence the tube developed for a considerable distance exclusively within the Quaternary age lava flow successions.

The gentle paleo-topography of the north-eastern part of the island at the time of the tube formation favoured a prolonged contact between pre-existing lava flows and the molten lava flowing through them. This prolonged contact led to the melting of the tube bed while knickpoints developed at slope changes favoured processes of thermo-mechanical erosion and so promoted the downcutting of the tube footwall.

To summarise, we infer that multiple causes operate in the placement and evolution of a large scale inflated lava tube. Through a combination of field work, three-dimensional reconstruction and geochemical analysis, it was possible to determine that the La Corona lava tube was emplaced among Quaternary lava flows generated during Los Helechos and La Corona activity and that the development of such huge dimensions was due to a combination of several concurrent conditions. The presence of a weak pyroclastic layer between pre-existing piled up lava flows facilitated the incipient inflation of lava in small sized tubes, whereas the gentle slope of the paleo-topography and the presence of knickpoints favoured lava tube entrenchment, the formation of tube-in-tube structures and the breakdown of the ceiling or the floor of different tube levels forming a unique tube section. All of these findings and parameters will be useful for future studies of pyroducts, not only on Earth, but also on other bodies in the Solar System such as the Moon and Mars where lava tubes have been widely documented and layers of weak material (regolith or soils) in-between lava flows are thought to be common.

Acknowledgments

We are grateful to the Cabildo de Lanzarote and the Geopark of Lanzarote and Archipelago Chinijo for granting permissiton to access and collect samples in the La Corona lava tube system and to the Spanish Geological Service for providing us with Lanzarote’s DTM. ESA-PANGEA partially supported this project with field activity and samples collection whereas GMAP-EPN2024 provided the tools for the digital geological mapping. LEICA geosystem provided the laser scan data of some sections of the tube realized through mobile mapping system during the PANGAEA-X 2017 campaign. We are grateful to Christophe Cloquet (SARM) for having performed the major and trace element analyses of our samples. We are grateful to Kaj Hoernle and Craig Lundstrom for sharing with us the locations of their samples, to Robbie Shone for his wonderful photos, and to Leonardo Tauro e Nicola Michelon for their technical support. We acknowledge the Vulcan Vertical Espeleologias y Barrancos speleo-group made their cave-surveys available and supported

us during the underground exploration.We acknowledge the careful english and scientific review by Dr Simon Crowhurst, from the Department of Geosciences at Cambridge University.
Finally, we acknowledge the two reviewers, David A. Williams and Laszlo P. Keszthelyi, for the really useful suggestions and discussions.

Data Availability Statement

The datasets analyzed during the current study are provided as tables within the paper or within the accompanying online material file. In addition, the full geochemical dataset, coordinates of samples and surface LIDAR are available open access at this repository link: https://doi.org/10.5281/zenodo.6572985.
The full 3D model dataset of the La Corona lava tube is property of the Virtual Geographic Agency (VIGEA) and is available under restricted access at the following repository link: https://doi.org/10.5281/zenodo.6573250. In order to protect the intellectual and commercial property of the La Corona lava tube 3D models, the entire dataset will be made accessible through the request access form in Zenodo. Access will be granted when the requester will state in written that the dataset will be used only for scientific research, excluding any commercial use.

References

Abdel-Monem, A., Watkins, N. D., and Gast, P. W. (1971). Potassium-argon ages, volcanic stratigraphy, and geomagnetic polarity history of the Canary Islands; Lanzarote, Fuerteventura, Gran Canaria, and La Gomera. *American Journal of Science*, 271(5), 490-521. https://doi.org/10.1111/j.1095-8312.1993.tb00878.x

Allred, K., and Allred, C. (1997). Development and morphology of Kazumura cave, Hawaii. *Journal of Caves and Karst Studies*, 59, 67-80.

Ancochea Soto, E., Brandle, J. L., Cubas, C. R., Hernán, F., and Huertas Coronel, M. J. (1996). Volcanic complexes in the eastern ridge of the Canary Islands: the Miocene activity of the island of Fuerteventura. *Journal of Volcanology and Geothermal Research*, 70(3-4), 183-204. https://doi.org/10.1016/0377-0273(95)00051-8

Atkinson, A., Griffin, T. J., and Stephenson, P. J. (1975). A major lava tube system from Undara Volcano, North Queensland. *Bulletin Volcanologique*, 39(2), 266-293.

Bard, E., Hamelin, B., and Fairbanks, R. G. (1990). U-Th ages obtained by mass spectrometry in corals from Barbados: sea level during the past 130,000 years. *Nature*, 346(6283), 456-458.

Bauer, I., Kempe, S., and Bosted, P. (2013). Kahuenaha Nui, Hawaii, a Cave Developed in Four Different Lava Flows. In Proceedings, *16th International Congress of Speleology*, Brno, Czech Republic (Vol. 3, pp. 231-236).

Bravo, T. (1964). El volcán y el malpaís de la Corona: La Cueva de los Verdes y los Jameos (p. 31). Arrecife, Spain: Cabildo Insular de Lanzarote.

Bunnell, D. (Ed.). (2013). *Cave of Fire - inside America's Lava Tubes (2nd ed.).* National Speleological Society, Inc.

Cabrera Vega, L. L. (2010). Sedimentología, estratigrafía, dinámica sedimentaria y evolución de El Jable (Lanzarote). *Propuesta de gestión (Doctoral dissertation)*.

Calvari, S. and Pinkerton, H., (1999). Lava tube morphology on Etna and evidence for lava flow emplacement mechanisms. *Journal of Volcanology and Geothermal Research*, 90(3-4): 263-280. https://doi.org/10.1016/S0377-0273(99)00024-4

Carracedo, J. C., Day, S., Guillou, H., Badiola, E. R., Canas, J. A., and Torrado, F. P. (1998). Hotspot volcanism close to a passive continental margin: *The Canary Islands. Geological Magazine*, 135(5), 591-604. https://doi.org/10.1017/S0016756898001447

Carracedo, J. C., Singer, B., Jicha, B., Guillou, H., Rodríguez Badiola, E., Meco, J., Pérez Torrado, F.J., Gimeno, D., Socorro, J.S. and Láinez, A. (2003). La erupción y el tubo volcánico del Volcán Corona (Lanzarote, Islas Canarias). *Estudios Geológicos*, 59, 277-302

Chappell, J., and Shackleton, N. (1986). Oxygen isotopes and sea level. *Nature*, 324(6093), 137-140.

Chatterjee, A., and Raymahashay, B. C. (1998). Spheroidal weathering of Deccan Basalt: a three-mineral model. *Quarterly Journal of Engineering Geology and Hydrogeology*, 31(3), 175-179. https://doi.org/10.1144/GSL.QJEG.1998.031.P3.02

Coan, T. (1844). Letter of March 15, 1843 describing the Mauna Loa eruption of 1843. *Missionary Herald*.

Coello J., Cantagrel, J. M., Heman F., Fuster J. M., Ibarrola, E., Ancochea, E., Casquet, C., Jamond, C., Dfaz de Teran, J. R. and Cendrero A. (1992). Evolution of the eastem volcanic ridge of the Canary Islands based on new K-Ar data. l. *Volcanol. Geotherm. Res.*, 53, 1-4: 251-274. https://doi.org/10.1016/0377-0273(92)90085-R

Cooper, K. M., and Kauahikaua, J. P. (1992). Morphology of extinct lava tubes and the implications for tube evolution, Chain of Craters Road, Hawaii Volcanoes National Park, Hawaii (pp. 1-44). US Geological Survey.

Cushing, G. E. (2012). Candidate cave entrances on Mars. *Journal of Cave and Karst Studies*, 74(1), 33-47. DOI: 10.4311/ 2010EX0167R

Dañobeitia, J. J., and Canales, J. P. (2000). Magmatic underplating in the Canary Archipelago. *Journal of Volcanology and Geothermal Research*, 103(1-4), 27-41. https://doi.org/10.1016/S0377-0273(00)00214-6

Detay, M., Gilli E., Gilli P., Hróarsson B. (2011). Volcanospéléologie En Islande perspectives scientifiques et émergence du géotourisme. LAVE. *Liaison des amateurs de volcanologie européenne*, (148), 18-31.

Dóniz Páez, J., Armas Ayala, V. y Romero, C. (2002). Unidades geomorfológicas del macizo volcánico antiguo de Famara (Lanzarote, Islas Canarias). En Pérez-González, A., Vegas, J. y Machado, M. (eds). Aportaciones a la geomorfología de España en el tercer milenio. *IGME*. Vol. 7. Ministerio de Ciencia y Tecnología. Madrid. 385-394.

Duncan, R. A. (1984). Age progressive volcanism in the New England seamounts and the opening of the central Atlantic Ocean. *Journal of Geophysical Research: Solid Earth*, 89(B12), 9980-9990. https://doi.org/10.1029/JB089iB12p09980

Francis, P. (1993) *Volcanoes: A Planetary Perspective*. Clarendon Press, Oxford University.

Gaina, C., Torsvik, T. H., van Hinsbergen, D. J., Medvedev, S., Werner, S. C., and Labails, C. (2013). The African Plate: A history of oceanic crust accretion and subduction since the Jurassic. *Tectonophysics*, 604, 4-25. https://doi.org/10.1016/j.tecto.2013.05.037

Gómez-Ulla, A., Sigmarsson, O., Huertas, M. J., Devidal, J. L., and Ancochea, E. (2018). The historical basanite-alkali basalt-tholeiite suite at Lanzarote, Canary Islands: Carbonated melts of heterogeneous mantle source? *Chemical Geology*, 494, 56-68. https://doi.org/10.1016/j.chemgeo.2018.07.015

Greeley, R. (1971a). Lava tubes and channels in the lunar Marius Hills. *The Moon*, 3(3), 289-314.

Greeley, R. (1971b). Observations of actively forming lava tubes and associated structures, Hawaii, part 1. (No. NASA-TM-X-62014).

Greeley, R., and Hyde, J. H. (1972). Lava tubes of the cave basalt, Mount St. Helens, Washington. Geological Society of America Bulletin, 83(8), 2397-2418. https://doi.org/10.1130/0016-7606(1972)83[2397:LTOTCB]2.0.CO;2

Greeley, R. (1973). Mariner 9 photographs of small volcanic structures on Mars. *Geology*, 1(4), 175-180. https://doi.org/10.1130/0091-7613(1973)1<175:MPOSVS>2.0.CO;2

Greeley, R., and Spudis, P. D. (1981). Volcanism on mars. *Reviews of Geophysics*, 19(1), 13-41. https://doi.org/10.1029/RG019i001p00013

Greeley, R., Fagents, S.A., Harris, R.S., Kadel, S.D., Williams, D.A. and Guest, J.E., (1998). Erosion by flowing lava: Field evidence. *Journal of Geophysical Research: Solid Earth*, 103(B11), 27325-27345. https://doi.org/10.1029/97JB03543

Hansen Machìn, A. and Pérez Torrado F. (2005): «The island and its territory: volcanism in Lanzarote». Geomorphology in regions of environmental contrasts. Zaragoza, September 7-11, 2005. *Field Trip Guides*, 505-534.

Harter III, J. W. (1972). Morphological Classification of Lava Tubes. In Proceedings of the International Symposium on Vulcanospeleology and its Extraterrestrial Applications (pp. 74-85). *Western Speleological Survey with National Speleological Society*, Seattle, WA.

Haruyama, J., Hioki, K., Shirao, M., Morota, T., Hiesinger, H., van der Bogert, C. H., Miyamoto, H., Iwasaki, A., Yokota, Y., Ohtake, M. and Matsunaga, T. (2009). Possible lunar lava tube skylight observed by SELENE cameras. *Geophysical Research Letters*, 36(21). https://doi.org/10.1029/2009GL040635

Haruyama, J., Sawai, S., Mizuno, T., Yoshimitsu, T., Fukuda, S., and Nakatani, I. (2012). Exploration of lunar holes, possible skylights of underlying lava tubes, by smart lander for investigating moon (slim). *Transactions of The Japan Society for Aeronautical and Space Sciences, Aerospace Technology Japan*, 10(ists28), Pk_7-Pk_10. https://doi.org/10.2322/tastj.10.Pk_7

Hoernle, K., and Carracedo, J. C. (2009). Canary Islands geology. *Encyclopedia of Islands*, (133-143). University of California Press. https://doi.org/10.1525/9780520943728-032

Holik, J. S., Rabinowitz, P. D. and Austin, J. A. 1991. Effects of Canary hotspot volcanism on structure of oceanic crust off Morocco. *Journal of Geophysical Research* 96, 12039–67.

Hon, K. E. N., Kauahikaua, J. I. M., Denlinger, R., and Mackay, K. (1994). Emplacement and inflation of pahoehoe sheet flows: Observations and measurements of active lava flows on Kilauea Volcano, Hawaii. *Geological Society of America Bulletin*, 106(3), 351-370. https://doi.org/10.1130/0016-7606(1994)106<0351:EAIOPS>2.3.CO;2

Horz, F. (1985). Lava tubes-potential shelters for habitats. In *Lunar bases and space activities of the 21st century* (pp. 405-412).

Ibarrola, E., and Lopez Ruiz, J. (1967). Estudio petrográfico y químico de las erupciones recientes (Serie IV) de Lanzarote (Islas Canarias). *Estudios Geológicos*, 23, 203-213.

Ibarrola, M. E. (1970). Variability of basaltic magmas in the eastern and central Canary Islands. *Estudios Geológicos*, 26, 337-399.

Irvine, T. N., and Baragar, W. R. A. (1971). A guide to the chemical classification of the common volcanic rocks. *Canadian Journal of Earth Sciences*, 8(5), 523-548. https://doi.org/10.1139/e71-055

Isler, O. (1989) ‘1986 International expedition to the Tunel de la Atlantida’, *Caves and Caving*, 45, pp. 16-21.

Jarvis, R. A. (1995). On the cross-sectional geometry of thermal erosion channels formed by turbulent lava flows. *Journal of Geophysical Research: Solid Earth*, 100(B6), 10127-10140. https://doi.org/10.1029/95JB00027

Jones, M. R., Soule, S. A., Gonnermann, H. M., Le Roux, V., and Clague, D. A. (2018). Magma ascent and lava flow emplacement rates during the 2011 Axial Seamount eruption based on CO2 degassing. *Earth and Planetary Science Letters,* 494, 32-41. https://doi.org/10.1016/j.epsl.2018.04.044.

Kauahikaua, J., Cashman, K. V., Mattox, T. N., Heliker, C. C., Hon, K. A., Mangan, M. T., and Thornber, C. R. (1998). Observations on basaltic lava streams in tubes from Kilauea Volcano, island of Hawai'i. Journal of Geophysical Research: Solid Earth, 103(B11), 27303-27323.

Kempe, S., Bauer, I., Bosted, P., Coons, D., and Elhard, R. (2010). Inflationary versus crusted-over roofs of pyroducts (lava tunnels). In *Proceedings 14th International Symposium on Vulcanospeleology* (p. 93).

Kempe, S. (2012, March). Lava caves, types and development. In *Abstracts and Proceedings 15th International Symposium on Vulcanospeleology*, Hashemite University Zarka, Jordan (pp. 37-56).

Kempe, S., (2019) Volcanic rock caves, *Encyclopedia of Caves (3rd ed.).* Academic Press, pp. 1118-1127. https://doi.org/10.1016/B978-0-12-814124-3.00131-X

Kerr, R. C. (2001). Thermal erosion by laminar lava flows. *Journal of Geophysical Research: Solid Earth*, 106(B11), 26453-26465. https://doi.org/10.1029/2001JB000227

Keszthelyi, L., and Self, S. (1998). Some physical requirements for the emplacement of long basaltic lava flows. *Journal of Geophysical Research: Solid Earth*, 103(B11), 27447-27464. https://doi.org/10.1029/98JB00606

Klitgord, K. D., and Schouten, H. (1986). Plate kinematics of the central Atlantic. The western north Atlantic region. *The Decade of North American Geology*, 1000, 351-378. DOI: https://doi.org/10.1130/DNAG-GNA-M.351

Labeyrie, L. D., Duplessy, J. C., and Blanc, P. L. (1987). Variations in mode of formation and temperature of oceanic deep waters over the past 125,000 years. *Nature*, 327(6122), 477-482.

Le Bas, M. J., Maitre, R. L., Streckeisen, A., Zanettin, B., and IUGS Subcommission on the Systematics of Igneous Rocks. (1986). A chemical classification of volcanic rocks based on the total alkali-silica diagram. *Journal of Petrology*, 27(3), 745-750. https://doi.org/10.1093/petrology/27.3.745

Lomoschitz, A., Marco, A. S., Huertas, M. J., Betancort, J. F., Isern, A., Sanz, E., and Meco, J. (2016). A reappraisal of the stratigraphy and chronology of Early Pliocene palaeontological sites from Lanzarote Island containing fossil terrestrial animals. *Journal of African Earth Sciences*, 123, 338-349. https://doi.org/10.1016/j.jafrearsci.2016.08.006

Luis, M. and Quirantes, S. F. (1984). El paisaje vegetal del malpaís de La Corona. *Revista de Geografía Canaria*, 1,105-128. Universidad de la Laguna.

Lundstrom, C. C., Hoernle, K., and Gill, J. (2003). U-series disequilibria in volcanic rocks from the Canary Islands: plume versus lithospheric melting. *Geochimica et Cosmochimica Acta*, 67(21), 4153-4177. https://doi.org/10.1016/S0016-7037(03)00308-9

Martí, J., and Ernst, G. G. (Eds.). (2008). *Volcanoes and the Environment*. Cambridge University Press.

Meco, J., Petit-Maire, N., Guillou, H., Carracedo, J. C., Lomoschitz, A., Ramos, A. G., and Ballester, J. (2003). Climatic changes over the last 5,000,000 years as recorded in the Canary Islands. *Episodes*, 26(2), 133-134.

Mendo, A., and Ortega, L. (1988). El túnel de La Atlántida. *Geo*, 14, 9-25.

Meyzen, C. M., Massironi, M., Pozzobon, R., and Dal Zilio, L. (2015). Are terrestrial plumes from motionless plates analogues to Martian plumes feeding the giant shield volcanoes? *Geological Society, London, Special Publications*, 401(1), 107-126. https://doi.org/10.1144/SP401.8

Montoriol-Pous, J., and De Mier, J. (1969). Estudio morfogenetico de las cavidades volcanicas desarrolladas en el malpais de la Corona (Isla de Lenzarote, Canarias). *Karst*, 6, 22.

Morgan, W. J. (1983). Hotspot tracks and the early rifting of the Atlantic. *In Developments in Geotectonics* (Vol. 19, pp. 123-139). Elsevier. https://doi.org/10.1016/B978-0-444-42198-2.50015-8

Ollier, C. D. (1971). Causes of spheroidal weathering. *Earth-Science Reviews*, 7(3), 127-141. https://doi.org/10.1016/0012-8252(71)90005-5

Pasquarè, G., Bistacchi, A., Francalanci, L., Bertotto, G. W., Boari, E., Massironi, M., and Rossotti, A. (2008). Very long pahoehoe inflated basaltic lava flows in the Payenia Volcanic Province (Mendoza and La Pampa, Argentina). *Revista de la Asociación Geológica Argentina*, 63(1), 131-149.

Peterson, D. W., Holcomb, R. T., Tilling, R. I., and Christiansen, R. L. (1994). Development of lava tubes in the light of observations at Mauna Ulu, Kilauea Volcano, Hawaii. *Bulletin of Volcanology*, 56(5), 343-360. doi: 10.1007/BF00326461

Roeser, H. A. (1982). Magnetic anomalies in the magnetic quiet zone off Morocco. In *Geology of the northwest African continental margin* (pp. 61-68). Springer, Berlin, Heidelberg. DOI: 10.1007/978-3-642-68409-8_4

Roest, W. R., Verhoef, J., and Pilkington, M. (1992). Magnetic interpretation using the 3-D analytic signal. *Geophysics*, 57(1), 116-125. https://doi.org/10.1190/1.1443174

Santin, S. F. (1969). Pegmatitoides in the horizontal basalts (series I) of Lanzarote and Fuerteventura Islands. *Bulletin Volcanologique*, 33(4), 989-1007. https://doi.org/10.1007/BF02597705

Sauro, F., Pozzobon, R., Santagata, T., Tomasi, I., Tonello, M., Martínez-Frías, J., Smets, L.M.J., Gómez, G.D.S. and Massironi, M. (2019). Volcanic Caves of Lanzarote: A Natural Laboratory for Understanding Volcano-Speleogenetic Processes and Planetary Caves. In *Lanzarote and Chinijo Islands Geopark: From Earth to Space* (pp. 125-142). Springer, Cham. DOI: 10.1007/978-3-030-13130-2_9

Sauro, F., Pozzobon, R., Massironi, M., De Berardinis, P., Santagata, T., and De Waele, J. (2020). Lava tubes on Earth, Moon and Mars: A review on their size and morphology revealed by comparative planetology. *Earth-Science Reviews*, 103288. https://doi.org/10.1016/j.earscirev.2020.103288

Shick, H. (2017). *Understanding lava tubes and lava caves (Amended 2nd ed.)*. Kazumura Cave Tours, Volcano, Hawaii.

Silver, P. G., Russo, R. M., and Lithgow-Bertelloni, C. (1998). Coupling of South American and African plate motion and plate deformation. *Science*, 279(5347), 60-63. DOI: 10.1126/science.279.5347.60

Smith, C. (2010) ‘A Cavers Guide to Lava Tubes of Lanzarote’, *Las Naturalistas*.

Sun, S. S., and McDonough, W. F. (1989). Chemical and isotopic systematics of oceanic basalts: implications for mantle composition and processes. *Geological Society, London, Special Publications*, 42(1), 313-345. https://doi.org/10.1144/GSL.SP.1989.042.01.19

Thomas, L. E., Hawkesworth, C. J., Van Calsteren, P., Turner, S. P., and Rogers, N. W. (1999). Melt generation beneath ocean islands: A U-Th-Ra isotope study from Lanzarote in the Canary Islands. *Geochimica et Cosmochimica Acta*, 63(23-24), 4081-4099. https://doi.org/10.1016/S0016-7037(99)00310-5

Titus, T. N., Wynne, J. J., Malaska, M. J., Agha-Mohammadi, A. A., Buhler, P. B., Alexander, E. C., ... and Wong, U. Y. (2021). A roadmap for planetary caves science and exploration. *Nature Astronomy*, 5(6), 524-525. https://doi.org/10.1038/s41550-021-01385-1

Torrese, P., Pozzobon, R., Rossi, A. P., Unnithan, V., Sauro, F., Borrmann, D., Lauterbach, H. and Santagata, T. (2021). Detection, imaging and analysis of lava tubes for planetary analogue studies using electric methods (ERT). *Icarus*, 357, 114244. https://doi.org/10.1016/j.icarus.2020.114244

van den Bogaard, P. (2013). The origin of the Canary Island Seamount Province-New ages of old seamounts. *Scientific Reports*, 3, 2107. DOI: 10.1038/srep02107

Water E. (2006). Recent Contributions to Icelandic Cave Exploration by the Shepton Mallet Caving Club (UK). *133 XII Symposium 2006, AMCS Bulletin*, (19), 188-196

Waters, A. C., Donnelly-Nolan, J. M., and Rogers, B. W. (1990). Selected caves and lava-tube systems in and near Lava Beds National Monument, California. *U.S. Geological Survey Bulletin 1673*. DOI: 10.3133/b1673

Wilkens, H., Iliffe, T. M., Oromí, P., Martínez, A., Tysall, T. N., and Koenemann, S. (2009). The Corona lava tube, Lanzarote: geology, habitat diversity and biogeography. Marine Biodiversity, 39(3), 155-167. DOI 10.1007/s12526-009-0019-2

Williams, D. A., Kerr, R. C., Lesher, C. M., and Barnes, S. J. (2001). Analytical/numerical modeling of komatiite lava emplacement and thermal erosion at Perseverance, Western Australia. *Journal of Volcanology and Geothermal Research*, 110(1-2), 27-55. https://doi.org/10.1016/S0377-0273(01)00206-2

Williams, D. A., Kadel, S. D., Greeley, R., Lesher, C. M., and Clynne, M. A. (2004). Erosion by flowing lava: geochemical evidence in the Cave Basalt, Mount St. Helens, Washington. *Bulletin of Volcanology*, 66(2), 168-181. DOI: 10.1007/s00445-003-0301-2

Williams, D. A., Kerr, R. C., and Lesher, C. M. (2011). Mathematical modeling of thermomechanical erosion beneath Proterozoic komatiitic basaltic sinuous rilles in the Cape Smith Belt, New Québec, Canada. *Mineralium Deposita*, 46(8), 943-958. DOI: 10.1007/s00126-011-0364-5

Wood, C. (1974). The genesis and classification of lava tube caves. *Transactions of the British Cave Research Association*, 1(1), 15-28.

References from the Supporting Information

Smith, J. V. (1998). Interpretation of domanial groundmass textures in basalt lavas of the southern Lamington Volcanics, eastern Australia. *Journal of Geophysical Research: Solid Earth*, 103(B11), 27383-27391. https://doi.org/10.1029/97JB03109

Captions:

Figure 1: Geological overview. a) Simplified map of the Canary Islands Seamount Provinces (CISP) location, including islands and associated seamounts, relative to Africa over the last 60 Ma. The stars track the location of the Canarian hotspot assuming a fixed position. Africa is held fixed to show relative motion of hotspot (Holik et al., 1991; Carracedo et al., 1998). At ~30 Ma, when the plate velocity drastically slows down (Gaina et al., 2013), the real position of the hotspot activity is significantly shifted from its predicted position. The archipelago construction stages do not reflect a regular progression in volcanism age toward the west. Ages in italic indicate the oldest dated subaerial volcanism of each island. b) Simplified geological map of Lanzarote. Red frame indicates the study area in the northern region of Lanzarote, while the red dashed line marks the path of La Corona lava tube. The geological unit contacts have been established from our study and earlier work by Hoernle and Carracedo (2009).

Figure 2: Reconstruction of the evolution of the East coast of Famara massif, in relation to the transgression-regression phases that allowed the formation and subsequent flooding of La Corona lava tube system: a) Erosion and excavation of the Mio-Pliocenic shield of Famara; b) Quaternary re-activation of the northern region. The lava flows of La Quemada and Los Helechos form a widespread lava field over the eroded plain of the Mio-Pliocenic shield; c) Eruption of the volcano La Corona and formation of the lava tube; d) The rising sea level, in the present interglacial, has left the submerged lava tube at the current level (modified from Carracedo et al., 2003); e) Simplified geological map of the northern region of Lanzarote. The map presents the locations of interest in the studied area in the municipality of Harìa (Lanzarote, Canary Islands) and the location of the collected samples.

Figure 3: Aerial and satellite images of the lava tube path. a) View of the eastern downslope of La Corona volcano taken from the secondary crater (see red star in b). The red circle marks the inflation sink position of the lava tube, while the white dashed line indicates the lava tube path. Large circular to elongated cavities in the background correspond to the Jameos. b) Plan-view of the lava field and skylights of the La Corona tube system. A) Jameos de los Molinos; B) Jameos de Arriba; C) Jameo de Francisco Leòn; D) Jameo de los Prendes; E) Jameo de la Gente; F) Jameo Tacho; G) Jameo Cumplido; H) Jameo Agujerado; I) Jameo de la Puerta Falsa; J) Jameo Redundo; K) Jameo de los Verdes; L) Jameo de los Lagos; M) Jameos del Agua (see also Supporting Information S1). The nomenclature adopted is updated, and sometimes differs from that used by Montoriol-Pous and De Mier, (1969). The dash-dotted black line highlights the topographic step at the base of the Famara massif.

Figure 4: Schematic cross-sections of the anchialine portions of La Corona lava tube system. A) Jameo de los Lagos, B) Cueva de los Lagos; C) Jameos del Agua lagoon (dash-dotted transversal lines indicate the areal extent occupied by the tourist complex); D) Túnel de la Atlántida (inset); E) Escondido lagoon; F) Dome room; G) Montaña de Arena "La Duna". Shaded areas in blue mark the position of current sea level. while horizontal dashed line indicates the possible sea level during tube formation. Vertical scale on left axis is exaggerated (modified from Wilkens et al., 2009). The zoomed section of Túnel de la Atlántida (D) is modified from Franjo Sànchez (https://franjosanchez.com/proyecto-sublantida/).

Figure 5: Views of the inner part of La Corona lava tube system: a) flow ledge (or bench) and, at the floor level, a small tube-in-tube structure (ph. Robbie Shone); b) cupola; c) window: an opening

between two conduits (ph. Gustavo D. Santana Gomez); d) multi-level structures (or tube-in-tube structures). The formation of a new secondary roof is often due to lava overflow into upper levels through windows, leaving deposits along the flow ledges that can grow and eventually seal the windows.

Figure 6: Sample locations along transversal sections of the tube and red lapilli layer identified as marker level inside the lava tube system: a) upstream branch of the Jameo de los Prendes - see section 1.03 in Plate 1, Supporting Information S1; b) downstream branch from the Jameo de los Prendes to Jameo de la Gente – see section 1.26 in Plate 1, Supporting Information S1; c) upstream branch from the Jameo de la Puerta Falsa to Jameo de la Gente – see section 2.06 in Plate 2, Supporting Information S1; d) Deposit of fallout material due to the initial Strombolian activity of La Corona volcano; e) the red layer is often covered by the lining walls and is exposed by the breaking down of those latter; f) exposed outcrop below the flow ledge in Jameo de la Puerta Falsa. The inset shows a zoom in of the outcrop.

Figure 7: Paleo-topography reconstruction. a) Surface reconstruction of the paleo-topography based on the position of the red pyroclastic level; b) Simulation of the interaction between the reconstructed surface and the current topography; c) Perpendicular section of the tube. Note that the reconstructed surface cuts the tube in several points. All reconstructions are done by using Cloud Compare software.

Figure 8: Major element variations (wt %) vs MgO (wt %) for lavas from the northern region of Lanzarote including samples from this work and those of Carracedo et al., (2003). Fields have been drawn from literature data of [1] Ibarrola and Lopez, 1968; [2] Santin, 1970; [3] Ibarrola, 1970; [4] Thomas et al., 1999; [5] Lundstrom et al., 2003; [6] Carracedo et al., 2003. All data were re-normalized to 100% (all iron as FeO^T).

Figure 9: Trace element concentrations in lavas from La Corona tube system normalized to the primitive-mantle values of Sun and McDonough (1989). Light green and dark green fields respectively denote data from Thomas et al. (1999) and Lundstrom et al. (2003).

Figure 10: Total alkalis vs SiO_2 (wt %) classification (TAS; Le Bas et al., 1986) for samples from the northern region of Lanzarote including samples collected for this study and those of Carracedo et al. (2003). Fields have been drawn from literature data [1] Ibarrola and Lopez, 1968; [2] Santin, 1970; [3] Ibarrola, 1970; [4] Thomas et al., 1999; [5] Lundstrom et al., 2003; [6] Carracedo et al., 2003.

Figure 11: Thermo-mechanical erosional stages of the lava tube in cross-sections. a) The primary effusive phase (C1) has covered the pyroclastic deposit of the initial Strombolian event; b) the inception of the tube by inflation (possibly by lava flows from either C1 or C2 units) starts exploiting the pyroclastic layer; c-d-e) progressive erosion and enlargement of the tunnel; f) post-cooling phase. On the walls are visible different layers of linings and flow ledges. The floor is covered by blocks and debris, remnants of the breaking down of the ceiling and lining walls.

Figure 12: Stages of La Corona volcano eruption. a) Volcanic products of the initial Strombolian event covering the area around the volcano. b) Effusive event C1 overlies the pyroclastic deposit. c) Opening of a secondary vent on the eastern side of the volcano. d) Formation of a lava pond at

the base of the volcano the hot lava starts to sink through the pre-existing lava flows down to the pyroclastic layer. e) Lava exploits the weakness of the pyroclastic level starting the excavation process. f) Post-cooling phase, the tube is drained. Collapses occur obstructing the access to the tube.

Table 1: Chemical analysis of samples from the pre-existing lava sequence of the tube walls and from Famara massif. Types of rocks: Bsn = Basanite; B-alk = Alkaline basalts; B-thl = Tholeiitic basalts.

Table 1

	Famara massif	**Los Helechos lava flows**		**La Corona lava flows**		**Lining walls lava flows**	
Samples	**CRB1**	**PL1**	**LPLB1**	**SUB1**	**LPUB1**	**PC1**	**LPCV1**
Type of rock*	Bsn	Bsn	Bsn	B-alk	B-thl	B-alk	B-alk
Major elements (wt. %)							
SiO_2	41.88	42.40	43.39	45.59	48.97	48.10	46.79
TiO_2	2.95	3.24	2.98	2.55	2.21	2.93	2.83
Al_2O_3	13.66	11.89	12.26	12.66	13.64	14.04	13.31
Fe_2O_{3T}	12.45	13.38	13.02	12.01	11.68	11.60	11.81
CaO	12.17	10.71	10.30	10.32	9.25	10.30	10.37
MgO	9.07	12.78	12.22	11.53	9.12	7.36	9.38
MnO	0.19	0.19	0.19	0.17	0.16	0.15	0.16
K_2O	0.51	0.46	0.99	0.76	0.64	0.87	1.02
Na_2O	3.25	3.45	3.39	3.03	3.24	3.62	3.29
P_2O_5	0.95	0.81	0.73	0.76	0.36	0.48	0.52
LOI	2.14	-0.09	0.10	-0.10	0.29	0.12	0.00
Total	99.232	99.22	99.55	99.27	99.55	99.56	99.47
Trace elemets (in ppm)							
Sc	29	26	25	24	22	24	25
V	273	269	259	241	189	307	532
Cr	310	488	533	491	355	313	401
Co	56	80	84	113	81	93	75
Ni	135	315	308	309	221	133	208
Cu	76	50	58	32	74	86	60
Zn	112	121	120	114	117	116	111
Ga	22	21	21	20	21	23	22
Cs	0.84	0.48	0.52	0.25	0.33	0.28	0.31
Rb	5.95	23.05	18.47	17.01	12.77	15.94	19.73
Ba	453	461	425	423	211	301	337
Th	7.33	8.24	7.51	8.92	3.75	5.60	6.05
U	1.91	1.99	2.15	2.47	1.06	3.16	1.89
Nb	76	67	60	58	28	49	49
Ta	5.33	4.93	4.30	3.75	2.05	3.88	3.67

Sr	929	853	820	856	490	671	752
Zr	393	270	242	211	153	269	225
Hf	7.71	6.29	5.55	4.64	3.73	6.25	5.34
La	58	54	50	58	23	36	40
Ce	127	110	101	114	49	74	81
Pr	15.19	12.90	11.87	13.18	6.05	8.87	9.56
Nd	60	51	47	51	26	36	38
Sm	11.56	9.90	9.37	9.80	6.19	7.99	8.03
Eu	3.49	3.04	2.91	3.00	2.08	2.58	2.55
Gd	9.13	7.91	7.55	7.84	5.51	6.88	6.81
Tb	1.21	1.07	1.02	1.06	0.80	0.95	0.94
Dy	6.50	5.66	5.53	5.67	4.48	5.18	5.08
Ho	1.17	1.01	0.97	0.99	0.81	0.92	0.90
Er	2.72	2.32	2.25	2.30	1.92	2.12	2.10
Tm	0.35	0.30	0.29	0.29	0.25	0.28	0.27
Yb	2.05	1.72	1.68	1.71	1.46	1.59	1.59
Lu	0.30	0.25	0.24	0.24	0.21	0.22	0.23
Y	30	25	25	25	21	23	24
Pb	2.34	2.42	2.21	2.15	1.34	2.08	2.15

***** Bsn = Basanite; B-alk = Alkaline basalts; B-thl = Tholeiitic basalts

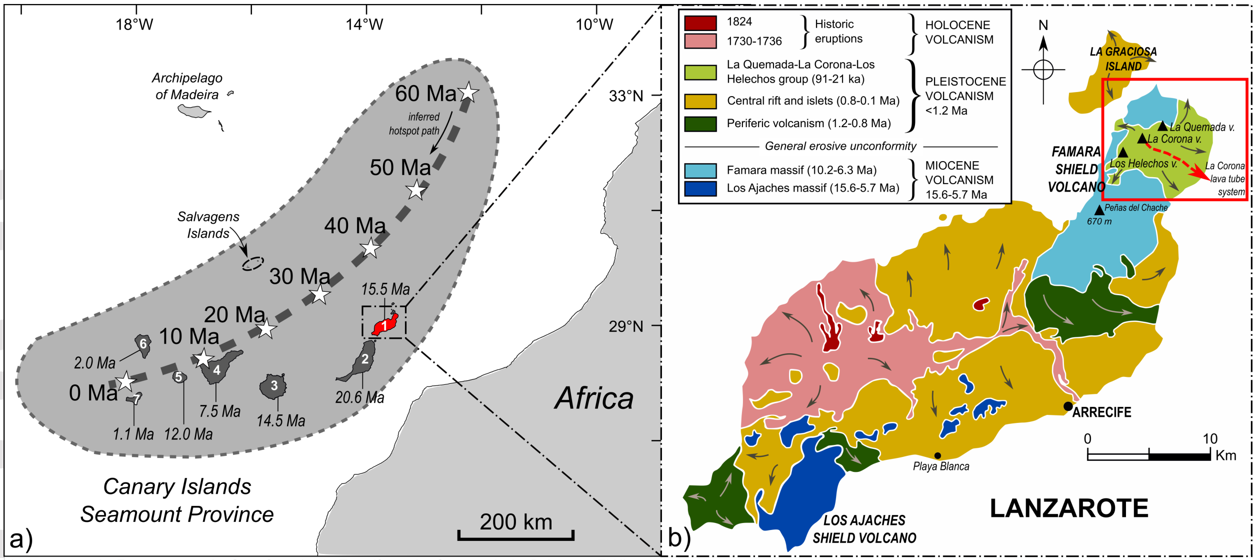

1 - Lanzarote, 2 - Fuerteventura, 3 - Gran Canaria, 4 - Tenerife, 5 - La Gomera, 6 - La Palma, 7 - El Hierro

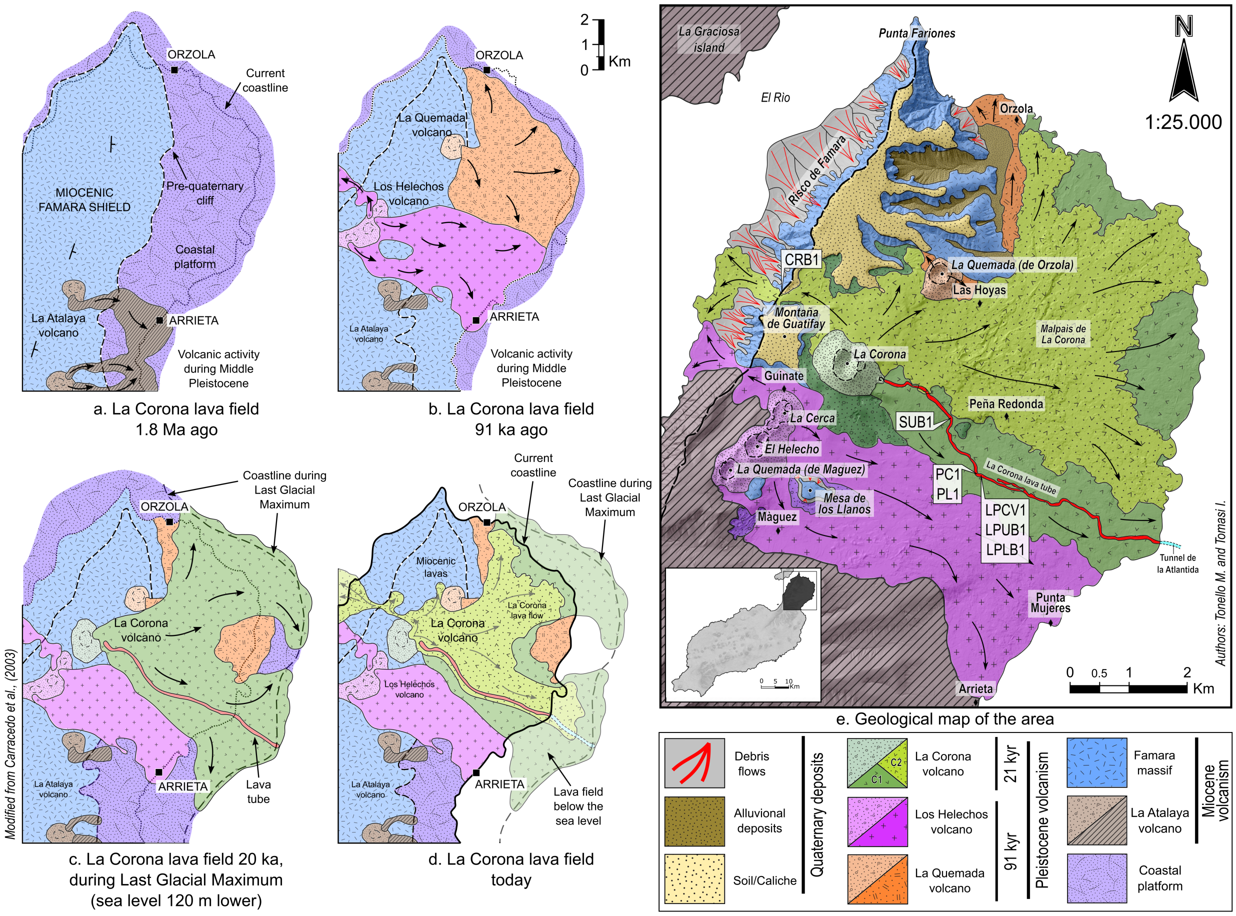

a. La Corona lava field 1.8 Ma ago

b. La Corona lava field 91 ka ago

c. La Corona lava field 20 ka, during Last Glacial Maximum (sea level 120 m lower)

d. La Corona lava field today

e. Geological map of the area

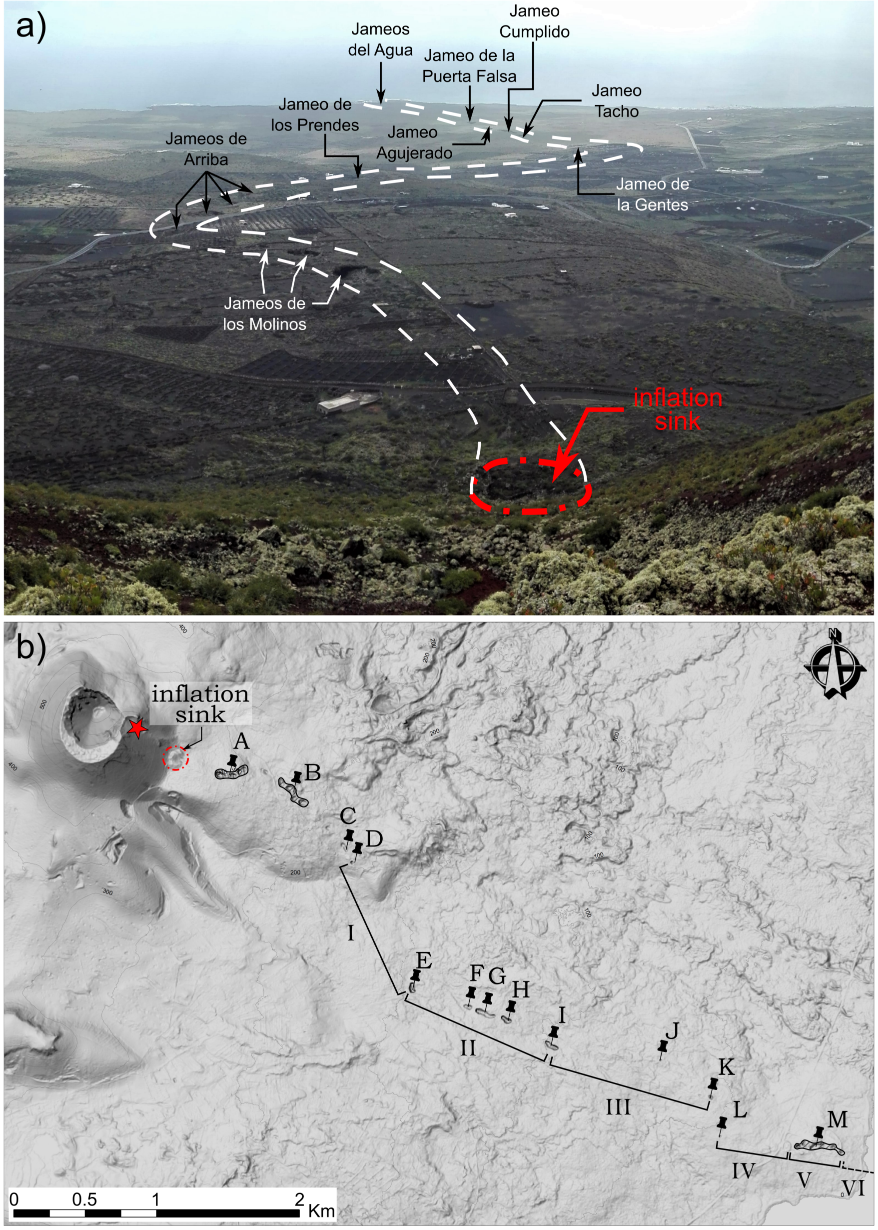
a)
Jameos del Agua
Jameo Cumplido
Jameo de la Puerta Falsa
Jameo Tacho
Jameo de los Prendes
Jameo Agujerado
Jameos de Arriba
Jameo de la Gentes
Jameos de los Molinos
inflation sink
b)
inflation sink
A
B
C
D
E
F
G
H
I
J
K
L
M
I
II
III
IV
V
VI
0
0.5
1
2
Km
N

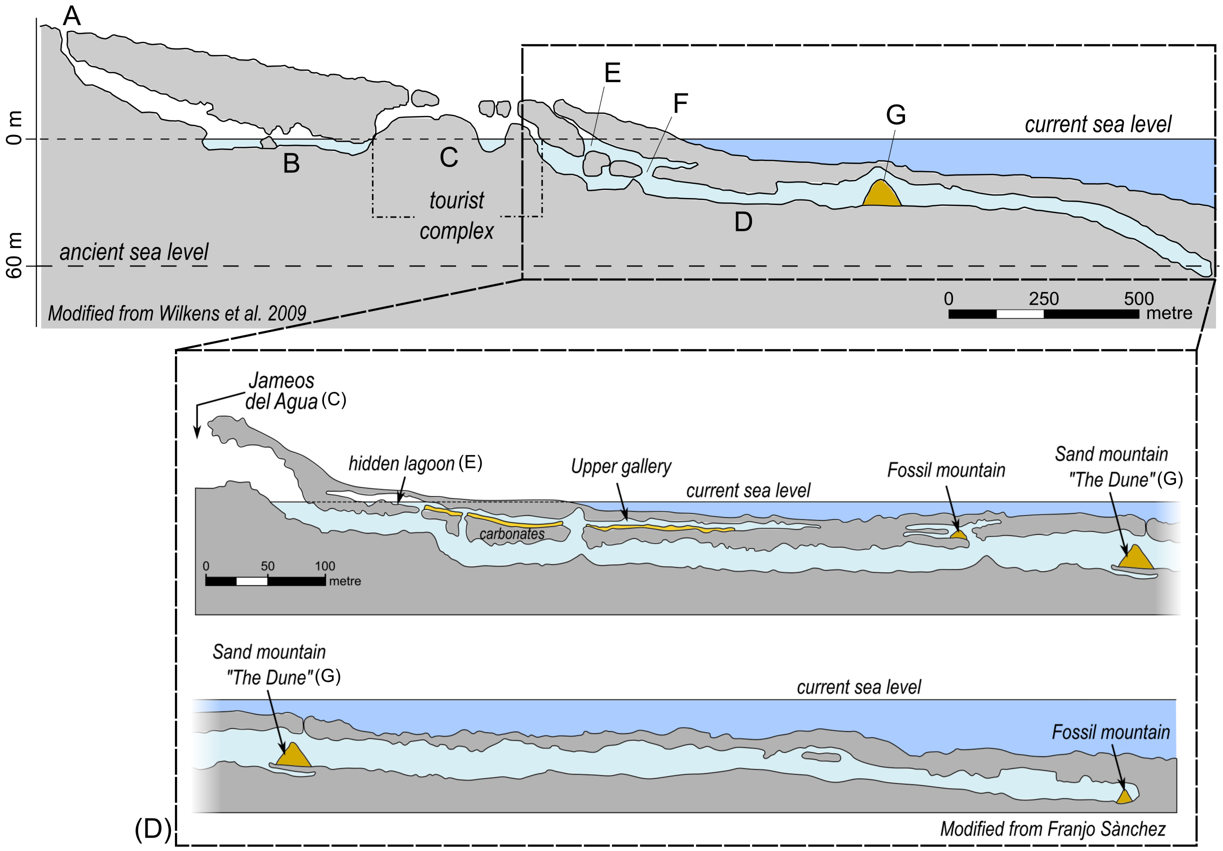
A
E
F
G
current sea level
0 m
B
C
tourist complex
D
60 m
ancient sea level
Modified from Wilkens et al. 2009
0 250 500 metre
Jameos del Agua (C)
hidden lagoon (E)
Upper gallery
current sea level
Fossil mountain
Sand mountain "The Dune" (G)
carbonates
0 50 100 metre
Sand mountain "The Dune" (G)
current sea level
Fossil mountain
(D)
Modified from Franjo Sànchez

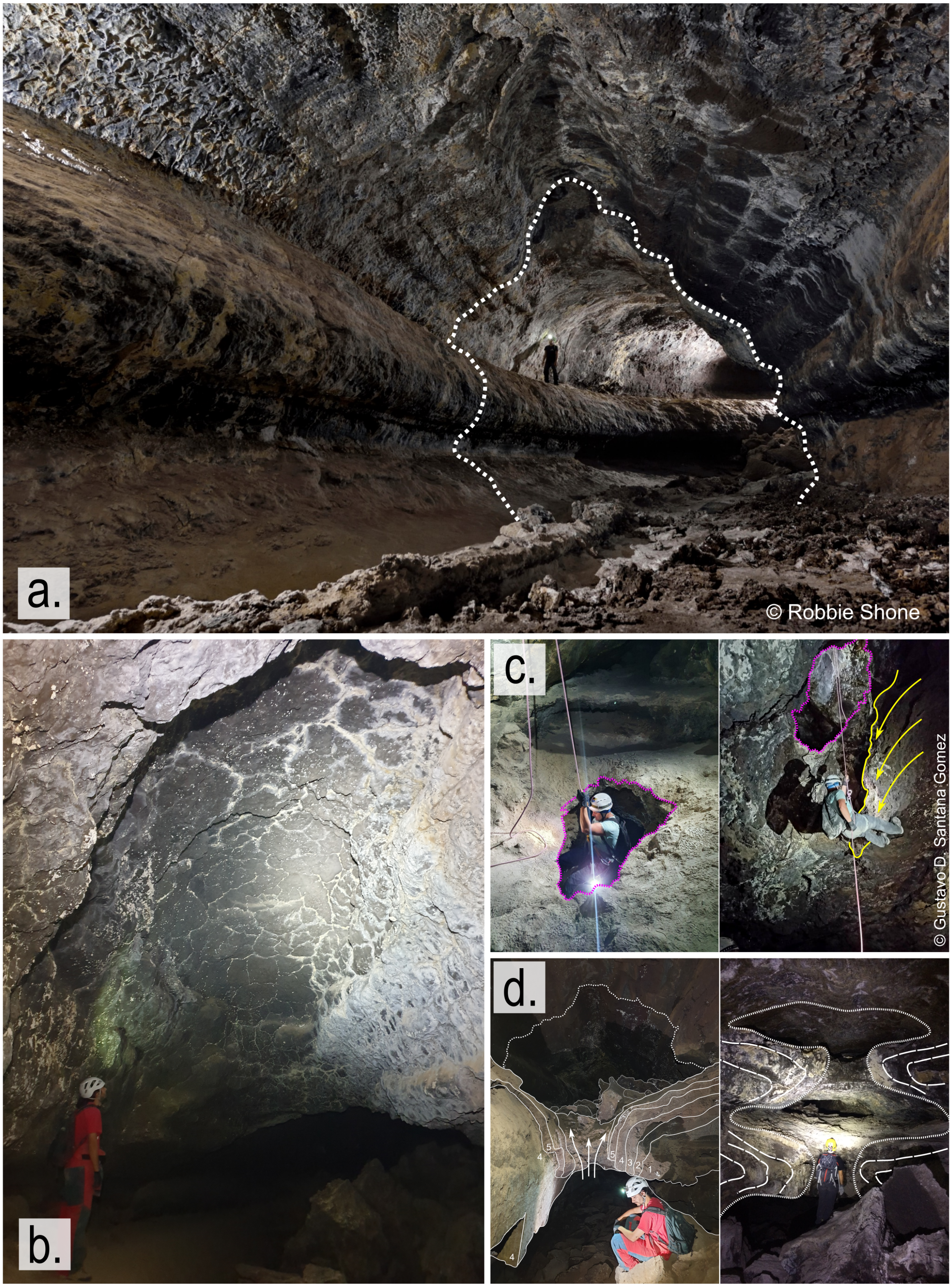
a.
© Robbie Shone
b.
c.
© Gustavo D. Santana Gomez
d.
5
4
5
4
3
2
1
4

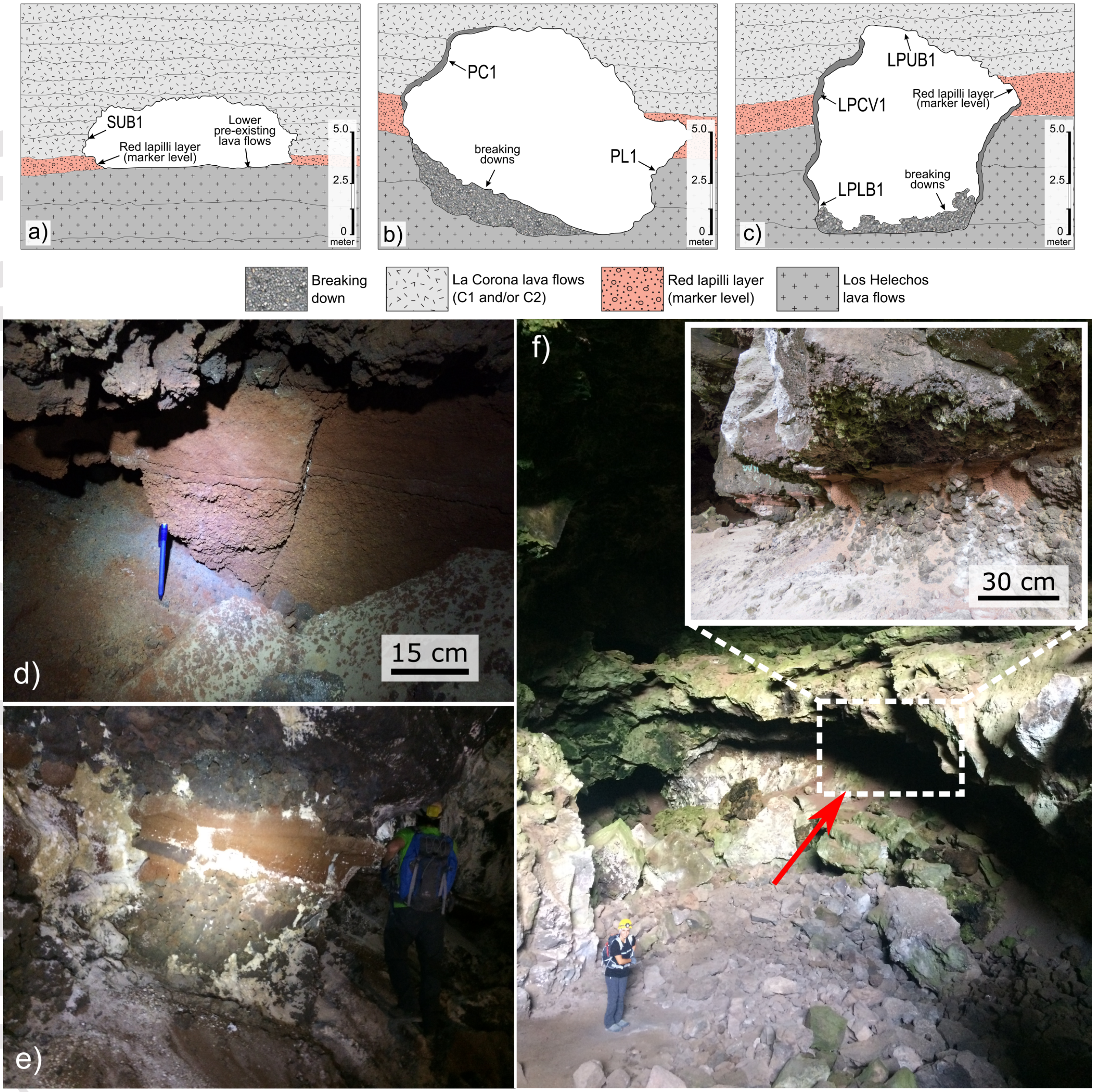
SUB1
Lower pre-existing lava flows
Red lapilli layer (marker level)
5.0
2.5
0
meter
a)
PC1
breaking downs
PL1
5.0
2.5
0
meter
b)
LPUB1
LPCV1
Red lapilli layer (marker level)
LPLB1
breaking downs
5.0
2.5
0
meter
c)
Breaking down
La Corona lava flows (C1 and/or C2)
Red lapilli layer (marker level)
Los Helechos lava flows
d)
15 cm
e)
f)
30 cm

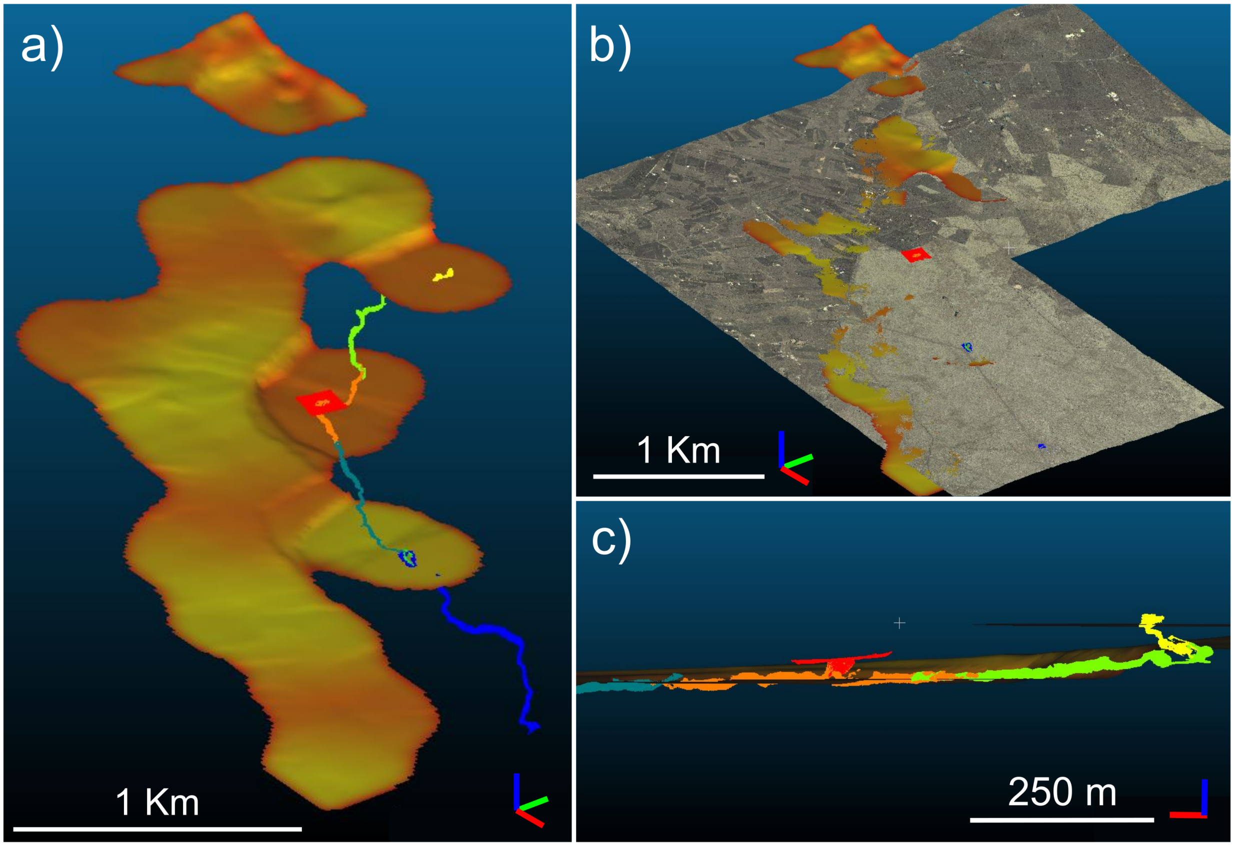
a)
1 Km
b)
1 Km
c)
250 m

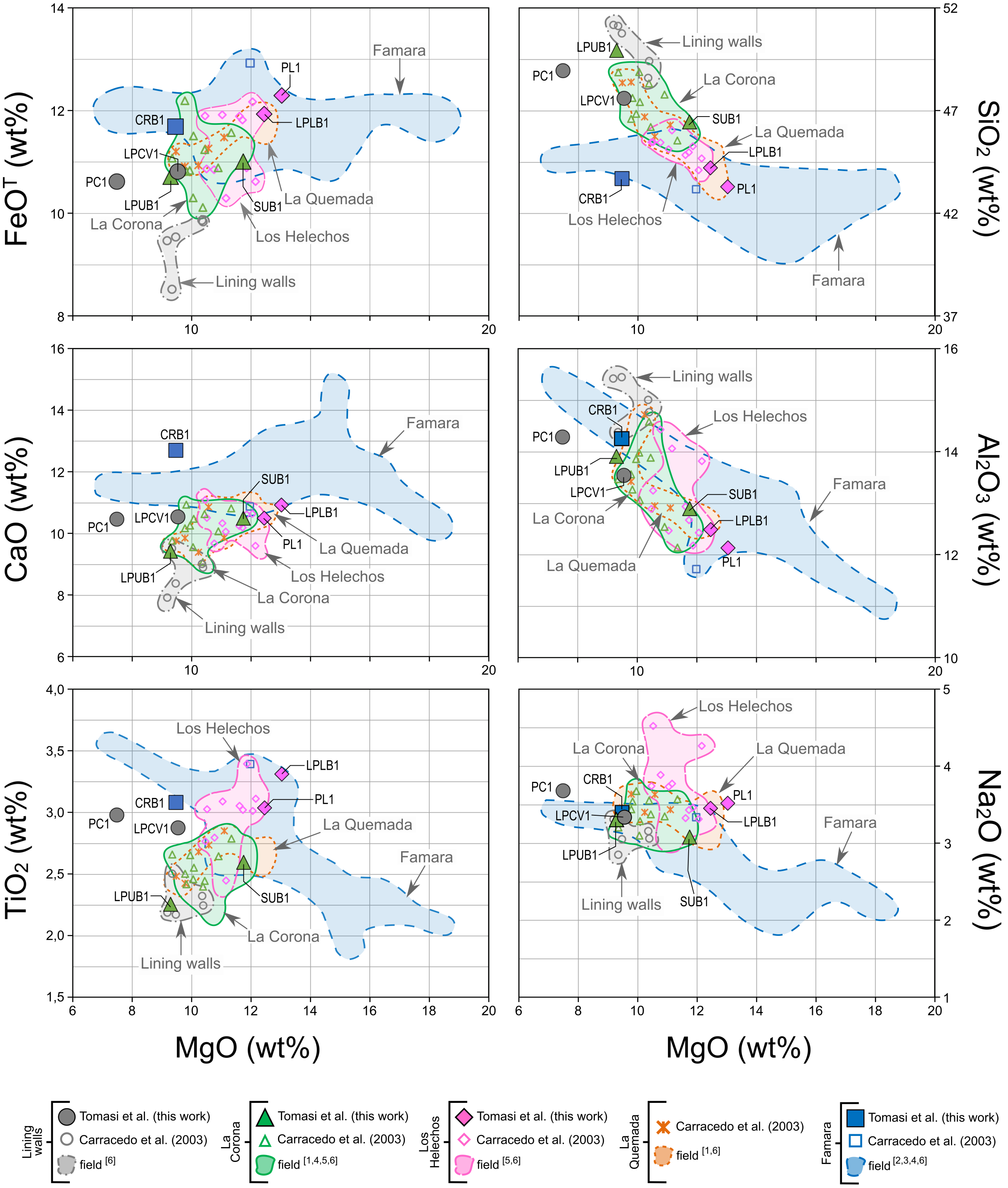
FeOT (wt%)
SiO2 (wt%)
CaO (wt%)
Al2O3 (wt%)
TiO2 (wt%)
Na2O (wt%)
MgO (wt%)
MgO (wt%)
14
12
10
8
52
47
42
37
16
14
12
10
8
6
16
14
12
10
4,0
3,5
3,0
2,5
2,0
1,5
5
4
3
2
1
6
8
10
12
14
16
18
20
Famara
Lining walls
La Corona
La Quemada
Los Helechos
PL1
LPLB1
CRB1
LPCV1
PC1
LPUB1
SUB1
Lining walls
Tomasi et al. (this work)
Carracedo et al. (2003)
field [6]
La Corona
Tomasi et al. (this work)
Carracedo et al. (2003)
field [1,4,5,6]
Los Helechos
Tomasi et al. (this work)
Carracedo et al. (2003)
field [5,6]
La Quemada
Carracedo et al. (2003)
field [1,6]
Famara
Tomasi et al. (this work)
Carracedo et al. (2003)
field [2,3,4,6]

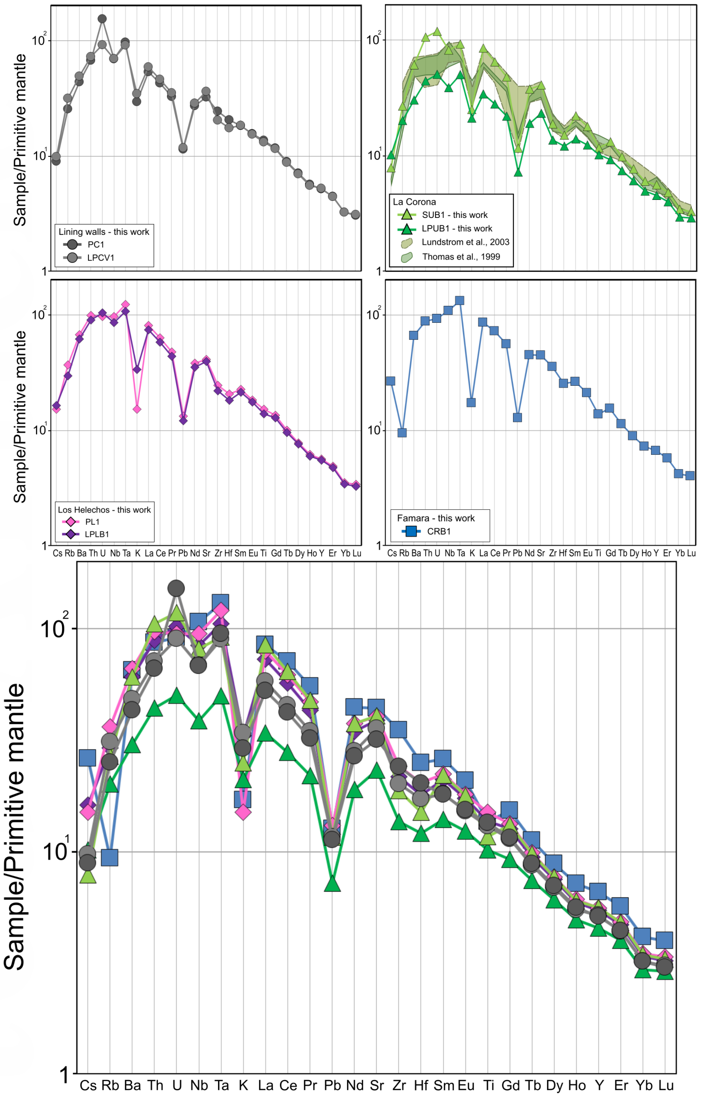
Sample/Primitive mantle
10²
10¹
1
Lining walls - this work
PC1
LPCV1
La Corona
SUB1 - this work
LPUB1 - this work
Lundstrom et al., 2003
Thomas et al., 1999
Los Helechos - this work
PL1
LPLB1
Famara - this work
CRB1
Cs Rb Ba Th U Nb Ta K La Ce Pr Pb Nd Sr Zr Hf Sm Eu Ti Gd Tb Dy Ho Y Er Yb Lu

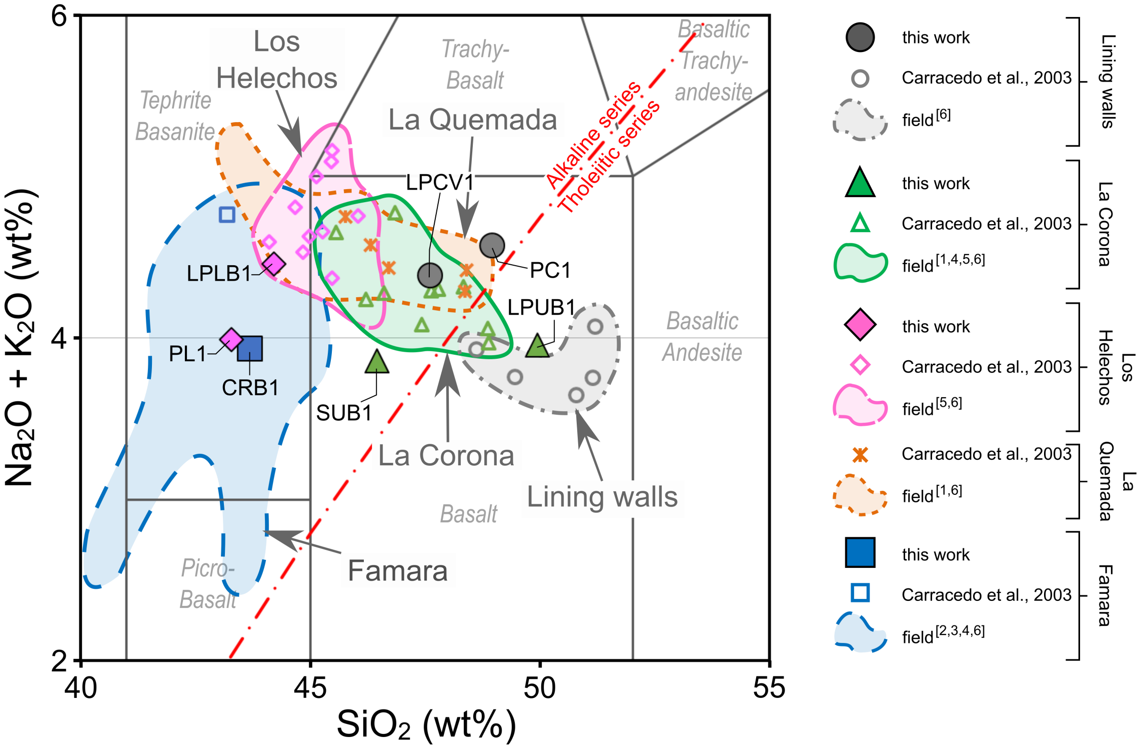
6
4
2
40
45
50
55
Na$_2$O + K$_2$O (wt%)
SiO$_2$ (wt%)
Tephrite Basanite
Trachy-Basalt
Basaltic Trachy-andesite
Basaltic Andesite
Basalt
Picro-Basalt
Alkaline series
Tholeiitic series
Los Helechos
La Quemada
La Corona
Lining walls
Famara
LPCV1
PC1
LPLB1
LPUB1
PL1
CRB1
SUB1
this work
Carracedo et al., 2003
field[6]
Lining walls
this work
Carracedo et al., 2003
field[1,4,5,6]
La Corona
this work
Carracedo et al., 2003
field[5,6]
Los Helechos
Carracedo et al., 2003
field[1,6]
La Quemada
this work
Carracedo et al., 2003
field[2,3,4,6]
Famara

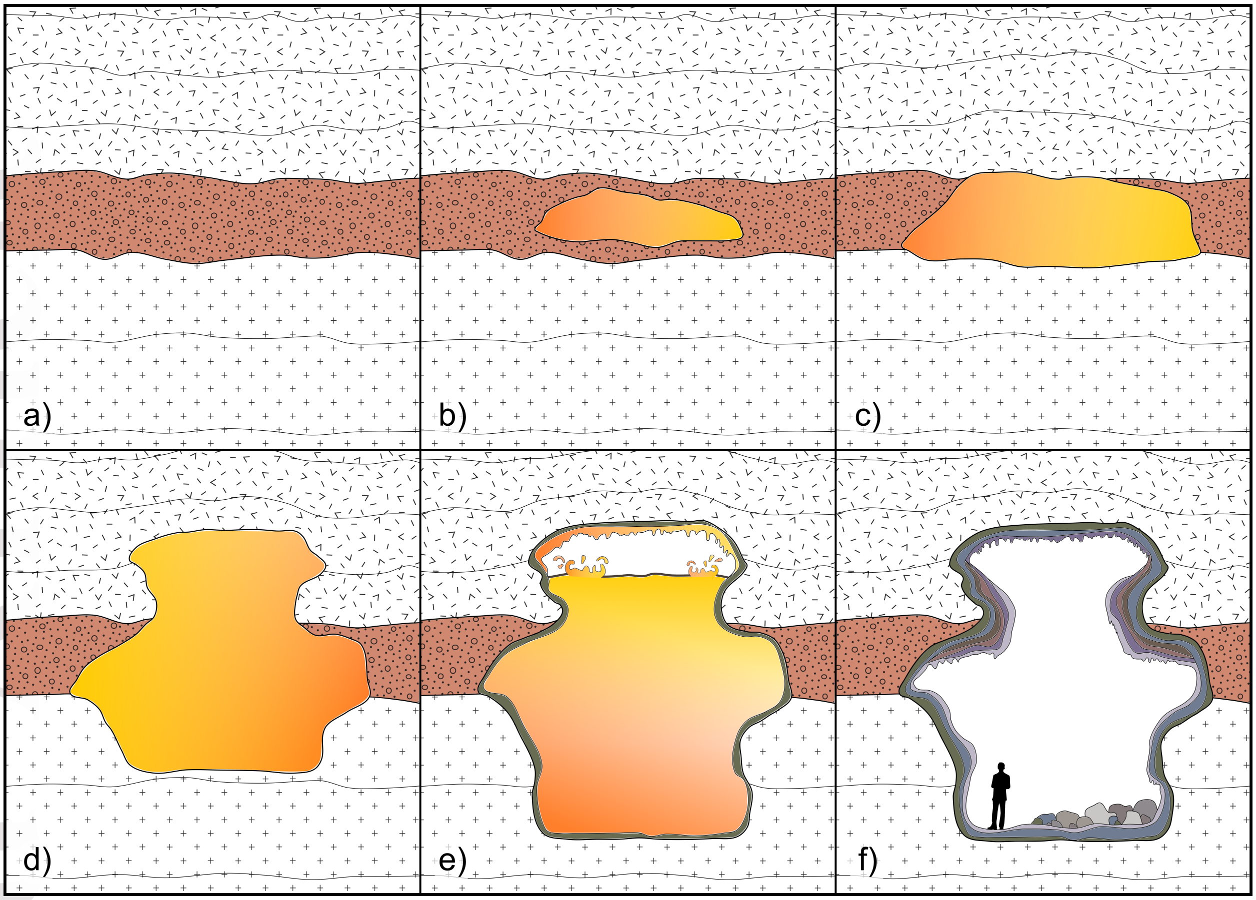
a)
b)
c)
d)
e)
f)

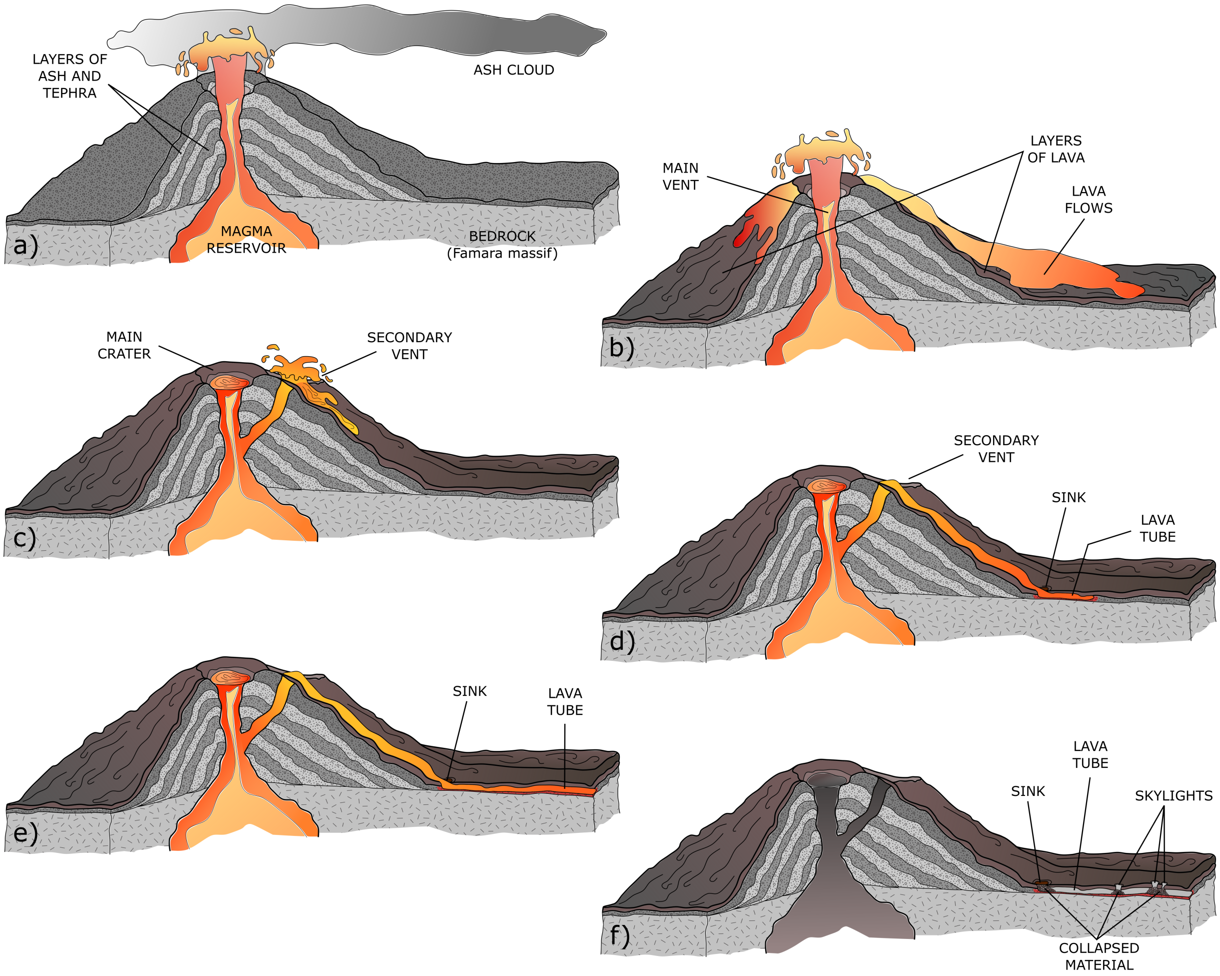
a)
LAYERS OF ASH AND TEPHRA
ASH CLOUD
MAGMA RESERVOIR
BEDROCK (Famara massif)
b)
MAIN VENT
LAYERS OF LAVA
LAVA FLOWS
c)
MAIN CRATER
SECONDARY VENT
d)
SECONDARY VENT
SINK
LAVA TUBE
e)
SINK
LAVA TUBE
f)
LAVA TUBE
SINK
SKYLIGHTS
COLLAPSED MATERIAL